Journal of Inorganic Biochemistry 195 (2019) 201–215

Contents lists available at ScienceDirect

Journal of Inorganic Biochemistry

journal homepage: www.elsevier.com/locate/jinorgbio

Binary-ternary Cd(II)-(hydroxycarboxylic acid)-(aromatic chelator) systems exhibit in vitro cytotoxic selectivity in a tissue-specific manner

O. Tsave[a], C. Iordanidou[a], C. Gabriel[a], A. Hatzidimitriou[b], A. Salifoglou[a,*]

[a] Laboratory of Inorganic Chemistry and Advanced Materials, Department of Chemical Engineering, Aristotle University of Thessaloniki, Thessaloniki 54124, Greece
[b] Laboratory of Inorganic Chemistry, Department of Chemistry, Aristotle University of Thessaloniki, Thessaloniki 54124, Greece

ARTICLE INFO

Keywords:
Cadmium hydroxy-isobutyric acid reactivity
Biotoxicity
Binary-ternary coordination polymers
Cell survival-death
Caspase
Cytoprotection

ABSTRACT

Cadmium is a metallotoxin, amply encountered in the environment and derived through physical and anthropogenic activities. Its entry in various organisms leads through water and the food chain to humans, thereby inducing a plethora of pathophysiologies. Delineation of the interactive role of cadmium with physiological and physiologically relevant substrates, requires well-defined forms of cadmium arising from such interactions along with the ensuing chemical reactivity amounting to toxic manifestations and health aberrations. To implement such efforts, low molecular mass substrate metal ion binders are needed, forming species with enhanced solubility and bioavailability. To that end, α-hydroxy isobutyric acid ($HIBAH_2$) was used in pH-specific synthetic efforts involving bulky aromatic chelators 2,2′-bipyridine (2,2′-bipy) and 1,10-phenanthroline (phen), thus leading to new crystalline materials $[Cd(C_4H_7O_3)_2]_n$(**1**), $[Cd(C_4H_7O_3)_2(H_2O)_2]$(**2**), $[\{Cd_2(C_4H_7O_3)_2(C_{10}H_8N_2)_2(H_2O)_2\}(NO_3)_2]_n{\cdot}nH_2O$(**3**), and $[\{Cd_2(C_4H_7O_3)_2(C_{12}H_8N_2)_2(H_2O)_2\}(NO_3)_2]_n{\cdot}2nH_2O$(**4**), which were physicochemically characterized (elemental analysis, FT-IR, NMR, ESI-MS, and X-ray crystallography) in the solid state and solution. Their physicochemical characteristics led to their employment in tissue-specific biological toxicity studies in three different cell lines. Their toxicity profile (cell viability, morphology, chemotacticity) was correlated through genetic biomarkers to apoptotic-necrotic processes, thereby shedding light on cadmium cellular toxicity processes. Finally, the cytoprotective action of specific chelators was examined, lending credence to the notion that appropriately structured chelators and antioxidants may be used as effective deterrent to cadmium toxicity. Collectively, structure-specificity linked to tissue-specific toxicity profiling in well-defined binary-ternary Cd(II)-$HIBAH_2$ systems exemplifies that metal ion's aberrant interactions in the cellular milieu, meriting further probing into the development of efficient chelators in cadmium detoxification.

1. Introduction

The increasing human exposure to toxic agents, derived mainly from anthropogenic activities over long periods of time, even at low doses, constitutes a major public health concern [1]. Cadmium (Cd) is one of the most known heavy metals [2]. Its consequences to human health during accumulation in ecosystems are catastrophic [3]. Cadmium is characterized by a long biological life (25 years) with an established toxicity profile [4,5]. Exposure to cadmium emerges from a) uncontrolled industrial waste disposal activities (e.g. paint and pigment factories, Ni—Cd batteries and fertilizer manufacturing, etc.) resulting in contaminated water and food chain, b) occupational exposure, and c) smoking [6–8]. Although the specific mechanism(s) of Cd(II)-induced toxicity are still debated, it is believed that Cd(II) uses the transport system of essential metals like zinc, calcium, and iron to enter cells. Through this way, it enters living beings and deregulates essential element homeostasis [9]. Subsequently, cadmium is absorbed by the liver and then accumulates in the kidneys. The liver and kidneys are considered as the major cadmium biotargets. The indirect promotion of Reactive Oxygen Species (ROS) production, which leads to Cd-induced oxidative stress and gradual cell damage or death, plays a major role [9–11]. Cadmium (Cd) is blamed for serious diseases, including aminoaciduria, proteinuria, renal tubular dysfunction, creatinuria [12], cardiovascular [13], skeletal-bone [12], respiratory, reproductive, and neurological [14] disorders. Itai-itai disease is such a disease related to cadmium's toxic impact on the food chain, characterized by severe pain, osteomalacia and bone decalcification [12]. Cadmium is considered a significant endocrine disruptor as well [15]. As a group I carcinogen [4,10,15], it affects cell division, proliferation, differentiation, apoptosis, and produces oxidative DNA damage,

* Corresponding author.
E-mail address: salif@auth.gr (A. Salifoglou).

https://doi.org/10.1016/j.jinorgbio.2019.02.009
Received 16 October 2018; Received in revised form 16 February 2019; Accepted 18 February 2019
Available online 23 February 2019
0162-0134/

chromosomal aberrations, and gene expression (p53, c-fos, c-jun, c-myc, etc.). [4,16–18]. Mobilization of Cd(II) in biofluids is of fundamental importance, closely associated with induced toxic manifestations. Coordination of the metallotoxin to organic binders in the cell or biological fluids, influences its solubility and mobilization, thereby promoting its toxic impact. Important such binders include α-hydroxycarboxylic acids with a significant biological role [12], providing many biological, pharmaceutical and nutritional products [19]. α-Hydroxy isobutyric acid ($HIBAH_2$) is a representative member of the class of α-hydroxycarboxylic acids, present in biological fluids (e.g. urine, saliva) as a) low molecular mass metabolites under (patho)physiological conditions, and b) important functional metal-coordinating agents, among others [12,19]. Paucity of well-defined binary and ternary Cd(II)-organic hydroxycarboxylic acid systems linked to the a) delineation of the toxicity of cadmium at the molecular level, and b) investigation of the associated molecular interactions between the specific metallotoxin and subcellular biotargets, prompted us to investigate the structural speciation of binary-ternary Cd(II)-(α-hydroxycarboxylic acid)-(N-donor) systems in aqueous media, thus leading to new well-defined hybrid materials. Physicochemical characterization of the new compounds led to the employment of select species in further investigation of their properties at the biological level. The pursued investigation of the relationship between structure and biological (toxic) effect on the well-defined cadmium species stands to contribute to the understanding of the role of structural speciation of cadmium in promoting biotoxicity. Implementation of such efforts involved in vitro work with tissue-specific cell lines, reflecting cellular processes (in)directly affected by cadmium. The so generated profile emerges essential in further pursuing development of preventive measures against cytotoxicity through a) antioxidant administration, and b) detoxification of the particular metallotoxin via appropriate selection of suitable sequestering chelators.

2. Experimental section

2.1. Materials and methods

All experimental procedures were carried out aerobically. The employed reagents (α-hydroxy isobutyric acid ($HIBAH_2$), 2,2′-bipyridine (2,2'-bipy), 1,10-phenanthroline (phen), KOH, NaOH, ammonia and piperazine) and solvents (nanopure water and ethanol) were purchased from commercial sources and used as obtained.

2.2. Physical measurements

FT-IR spectra were carried out on a Thermo Electron Nicolet IR 200 FT-Infrared spectrometer using KBr pellets. The simultaneous determination of carbon, hydrogen and nitrogen (%) took place in a Thermo Finnigan Flash EA 1112 CHNS elemental analyzer. The analyzer is based on the dynamic flash combustion of the sample at 1800 °C. Reduction, trapping, complete GC separation and product detection followed the combustion process. The instrument is fully automated and PC controlled via the Eager 300 software.

2.2.1. Solution NMR spectroscopy

Solution ^1H and ^{13}C NMR experiments for **1–4**, were carried out on a Varian 600 MHz spectrometer. The sample concentration was ~5 mM. Freshly prepared compounds were dissolved in D_2O. Carbon spectra were acquired with 5000 transients, a spectral width of 20,000 Hz and a relaxation delay of 2 s. Proton spectra were acquired with 2046 transients and a spectral width of 9000 Hz. Experimental data were processed using VNMR routines. Spectra were zero-filled and subjected to exponential apodization prior to FT. Chemical shifts (δ) are reported in ppm, while spectra were referenced by the standard experimental setup.

2.2.2. ESI-MS spectrometry

Electrospray ionization mass spectrometry (ESI-MS) infusion experiments were carried out on a ThermoFisher Scientific (Bremen, Germany) model LTQ Orbitrap Discovery MS. The $HIBAH_2$ ligand, (L_1H = ($C_4H_8O_3$), and compounds $[Cd(L)_2]_n$ (**1**), $[Cd(L)_2(H_2O)_2]$ (**2**), $[\{Cd_2(L)_2(C_{10}H_8N_2)_2(H_2O)_2\}(NO_3)_2]_n{\cdot}nH_2O$ (**3**) and $[\{Cd_2(L)_2(C_{12}H_8N_2)_2(H_2O)_2\}(NO_3)_2]_n{\cdot}2nH_2O$ (**4**) were dissolved in water and introduced into the ESI source of the MS through an integrated syringe pump, at a flow rate of 5 μL/min. The infusion experiments were run using a standard ESI source, operating in a positive ionization mode. Source operating conditions were a 3.7 kV spray voltage and a 320 °C heated capillary temperature.

2.2.3. Thermal studies

Thermogravimetric analysis was carried out in an aerobic atmosphere using a Perkin Elmer Pyris 1 TGA system. The heating rate was 5 °C/min, in the temperature range 25–900 °C, with the sample mass being in the range 2–10 mg. The sample weight loss was recorded continuously during the procedure in a dynamic fashion, as a function of temperature or time between 25 and 900 °C.

2.3. Synthesis

2.3.1. Synthesis of $[Cd(C_4H_7O_3)_2]_n$ (1)

Method A: A quantity of $Cd(NO_3)_2{\cdot}4H_2O$ (0.15 g, 0.50 mmol) was placed in a flask and dissolved in 10 mL of H_2O. Subsequently, 0.10 g (1.0 mmol) of α-hydroxy isobutyric acid ($HIBAH_2$) was added under continuous stirring. An aqueous solution of potassium hydroxide (0.1 N KOH) was employed to adjust the pH of the reaction mixture to the final value of 5. The resulting reaction solution was allowed to stir for 30 min and then placed at 4 °C, with addition of cold ethanol to the reaction solution taking place occasionally (every 3 days). After three weeks, colorless crystalline material appeared at the bottom of the vessel. The compound was isolated by filtration and air-dried at room temperature. The yield of the reaction was 0.060 g (~38%). **Anal. Calc.** for **1, [Cd($C_4H_7O_3$)$_2$]$_n$ (1)** ($C_8H_{14}CdO_6$, M_r: 318.60) (%) C: 30.10; H: 4.40. Found: C: 30.02; H: 4.41.

Method B: The same procedure as in **A** was followed. Addition of aqueous solution of ammonia, to adjust the pH of the reaction mixture to a final value of 5, led after slow evaporation of the solvent at room temperature to the isolation of the same crystalline material **1**. The yield of the reaction was 0.045 g (~28%).

Method C: Isolation of crystalline compound **1** took place upon slow evaporation, at room temperature, of the reaction solution containing $Cd(NO_3)_2{\cdot}4H_2O$:$HIBAH_2$, α-hydroxy isobutyric acid ($HIBAH_2$) (molar ratio 1:2) and addition of 1 mmol of piperazine to a final pH 3. The yield of the reaction was 0.030 g (~19%).

In all of the above cases, analytical and FT-IR spectroscopic data supplemented by X-day crystallography confirmed the identity of the derived compound **1**.

2.3.2. Synthesis of $[Cd(C_4H_7O_3)_2(H_2O)_2]$ (2)

$Cd(NO_3)_2{\cdot}4H_2O$ (0.15 g, 0.50 mmol) and α-hydroxy isobutyric acid ($HIBAH_2$) (0.10 g, 1.0 mmol) were dissolved in 15 mL of H_2O under continuous stirring. Subsequently, adjustment of pH took place to a final value of 5 with an aqueous solution of sodium hydroxide (0.1 N NaOH). The arising reaction mixture was transferred to a Teflon-lined stainless steel reactor (23 mL) and heated to 160 °C for 72 h (hydrothermal reaction). After cooling of the reactor to room temperature, the final resulting mixture was filtered under vacuum and the filtrate was left to evaporate slowly at room temperature. After twenty days, colorless crystals appeared at the bottom of the vessel, which were isolated by filtration and dried in the air. Yield: 0.065 g (40%). Anal. Calc. for **2**, **[Cd($C_4H_7O_3$)$_2$(H_2O)$_2$]** (**2**) ($C_8H_{18}CdO_8$, M_r: 354.63): C: 27.07; H: 5.07. Found: C, 27.19. H, 5.10.

Table 1
Summary of crystal, intensity collection and refinement data for $[Cd(C_4H_7O_3)_2]_n$ (**1**), $[Cd(C_4H_7O_3)_2(H_2O)_2]$ (**2**), $[\{Cd_2(C_4H_7O_3)_2(C_{10}H_8N_2)_2(H_2O)_2\}(NO_3)_2]_n{\cdot}nH_2O$ (**3**), and $[\{Cd_2(C_4H_7O_3)_2(C_{12}H_8N_2)_2(H_2O)_2\}(NO_3)_2]_n{\cdot}2nH_2O$ (**4**).

Compound	1	2	3	4
Chemical formula	$C_8H_{14}CdO_6$	$C_8H_{18}CdO_8$	$C_{28}H_{36}Cd_2N_6O_{15}$	$C_{32}H_{38}Cd_2N_6O_{16}$
M_r	318.60	354.63	921.42	987.48
Crystal system	Monoclinic	Monoclinic	Monoclinic	Monoclinic
Space group	$P2_1/c$	$C2/c$	$P2_1/c$	$P2_1/c$
Temperature (K)	295	295	293	295
a (Å)	7.9810(5)	10.2932(11)	41.904(5)	11.384(1)
b (Å)	8.0308(5)	5.7304(6)	11.5500(12)	24.095(2)
c (Å)	8.2182(5)	22.209(3)	15.1962(16)	15.2419(13)
β (°)	93.919(2)	101.477(2)	98.624(3)	111.518(2)
V (Å^3)	525.50(6)	1283.8(2)	7271.7(13)	3889.3(6)
Z	2	4	8	4
Radiation type	Mo $K\alpha$	Mo $K\alpha$	Mo $K\alpha$	Mo $K\alpha$
μ (mm^{-1})	2.08	1.73	1.24	1.17
Crystal size (mm)	0.14 × 0.1 × 0.09	0.22 × 0.19 × 0.14	0.26 × 0.24 × 0.17	0.34 × 0.27 × 0.19
Data collection				
Diffractometer	Bruker Kappa Apex2	Bruker Kappa Apex2	Bruker Kappa Apex2	Bruker Kappa Apex2
Absorption correction	Numerical	Numerical	Numerical	Numerical
T_{min}, T_{max}	0.80, 0.83	0.72, 0.79	0.74, 0.81	0.73, 0.80
Reflections				
No. of measured	3910	6715	71,683	199,410
Independent	1014	1367	14,837	8342
Observed [$I > 2.0\sigma(I)$]	895	1351	10,713	7416
R_{int}	0.020	0.010	0.017	0.020
(sin θ/λ)$_{max}$ (Å^{-1})	0.618	0.634	0.628	0.637
Refinement				
$R[F^2 > 2\sigma(F^2)]$	0.015	0.028	0.054	0.032
$R_w(F^2)$	0.027	0.030	0.084	0.055
S	1.00	1.00	1.00	1.00
No. of reflections	895	1351	10,713	7416
No. of parameters	70	78	919	499
H-atom treatment	H-atom parameters constrained	H-atom parameters constrained	H-atom parameters constrained	H-atom parameters constrained
Δρ$_{max}$, Δρ$_{min}$ (e Å^{-3})	0.28, −0.18	0.90, −2.08	2.13, −2.20	0.45, −0.58

$R = \frac{\sum ||F_o| - |F_c||}{\sum(|F_o|)}$, $R_w = \sqrt{\sum [w(F_o^2 - F_c^2)^2] / \sum [w(F_o^2)^2]}$.

2.3.3. Synthesis of $[\{Cd_2(C_4H_7O_3)_2(C_{10}H_8N_2)_2(H_2O)_2\}(NO_3)_2]_n{\cdot}nH_2O$ (3)

A quantity of $Cd(NO_3)_2{\cdot}4H_2O$ (0.15 g, 0.50 mmol) was dissolved in 15 mL of H_2O and α-hydroxy isobutyric acid ($HIBAH_2$) (0.10 g, 1.0 mmol) was added slowly under continuous stirring. Then, 2,2'-bipy (0.080 g, 0.50 mmol) was added to the reaction mixture and addition of an aqueous solution of sodium hydroxide (0.1 N NaOH) took place for the adjustment of pH to a final value > 8. The solution was left under stirring for 1/2 h and then placed in a 23 mL Teflon-lined stainless steel reactor to react hydrothermally at 160 °C for 72 h. Subsequently, the reactor was allowed to cool to room temperature and the resulting mixture was filtered under vacuum. The emerging filtrate was allowed to evaporate at room temperature. After three weeks, colorless crystalline material appeared. The resulting crystalline product was recovered by filtration and air-dried. Yield 0.11 g (~23%). Anal. Calc. for **3**, $[\{Cd_2(C_4H_7O_3)_2(C_{10}H_8N_2)_2(H_2O)_2\}(NO_3)_2]_n{\cdot}nH_2O$ (**3**). ($C_{28}H_{36}Cd_2N_6O_{15}$, M_r: 921.42) (%) C, 36.46; H, 3.90; N, 9.11. Found: C, 36.50; H: 3.92; N, 9.07.

2.3.4. Synthesis of $[\{Cd_2(C_4H_7O_3)_2(C_{12}H_8N_2)_2(H_2O)_2\}(NO_3)_2]_n{\cdot}2nH_2O$ (4)

A quantity of $Cd(NO_3)_2{\cdot}4H_2O$ (0.15 g, 0.50 mmol) was dissolved in 10 mL of H_2O under stirring. Subsequently, α-hydroxy isobutyric acid ($HIBAH_2$) (0.10 g, 1.0 mmol) was added to the reaction mixture. At the same time, a quantity of 1,10-phenanthroline (0.090 g, 0.50 mmol) was dissolved in a vessel containing 5 mL of CH_3OH and transferred to the aqueous reaction mixture of $Cd(NO_3)_2{\cdot}4H_2O$ and α-hydroxy isobutyric acid ($HIBAH_2$). The mixture was allowed to stir for 1/2 h. Addition of aqueous solution of ammonia (0.1 N) led to the adjustment of pH to a final value of > 8. The resulting cloudy reaction mixture was stirred for an additional 30 min. Addition of 2 mL of CH_3OH resulted in a clear solution. The emerging solution was then allowed to evaporate slowly at room temperature. Yellowish crystals appeared at the bottom of the vessel after several weeks. The crystalline material was recovered by filtration and air-dried. Yield 0.080 g (17%). Anal. Calc. for **4** $[\{Cd_2(C_4H_7O_3)_2(C_{12}H_8N_2)_2(H_2O)_2\}(NO_3)_2]_n{\cdot}2nH_2O$ ($C_{32}H_{38}Cd_2N_6O_{16}$, M_r: 987.48): (%) C, 38.78; H, 3.83; N, 8.48. Found: C, 39.00; H, 3.78; N, 8.40.

2.3.5. Transformation of 1 to 2

A quantity of the polymeric compound $\mathbf{[Cd(C_4H_7O_3)_2]_n}$ (**1**) (0.20 mmol, 0.060 g) was dissolved in 10 mL of H_2O. The solution was transferred in a 23 mL Teflon-lined stainless steel reactor and heated to 160 °C for 72 h. Upon return to room temperature, the resulting reaction mixture was filtered and evaporated slowly in the air at room temperature. Gradually, the color of the solution changed from colorless to yellowish and several weeks later a yellowish crystalline material appeared. The resulting crystalline product was recovered by filtration and air-dried. Yield: 0.065 g (40%). The crystalline product was identified as $\mathbf{[Cd(C_4H_7O_3)_2(H_2O)_2]}$ (**2**) by FT-IR spectroscopy and X-ray crystallographic determination of one of its isolated single crystals.

2.4. X-ray crystal structure determination

Single crystals of compounds **1–4** were taken from the mother liquor and placed on a Bruker Kappa 2 APEX diffractometer at room temperature, equipped with a triumph monochromator using Mo Ka radiation. Unit cell dimensions were determined and refined by using the

angular settings of at least 100 high intensity reflections ($> 10\ \sigma(I)$) in the range $20^\circ < 2\theta < 42^\circ$. Data collection was performed using φ and ω scans. No crystal decay was observed during data collection. The collected data were integrated with the Bruker SAINT software package [20] using a narrow-frame algorithm. Data were corrected for absorption using the numerical method SADABS, based on the crystal dimensions [21]. The structures were solved using SUPERFLIP [22], as implemented in the "Crystals" crystallographic package. Optimization of the data was performed by full matrix least squares on F^2 using Crystals version 14.61_build_6236 [23]. All non-hydrogen atoms were found and refined anisotropically except for the oxygen atoms of the nitrate counter ions in the structure of **4**. All hydrogen atoms were located at their expected positions. Finally, molecular illustrations were drawn by the Diamond 3.1 crystallographic package [24]. Crystallographic details of **1–4** complexes are summarized in Table 1.

2.5. Cell cultures and biological tests

2.5.1. Cell cultures

In the present study, in an effort to evaluate the biological profile of the newly synthesized materials, three cell lines, namely a) 3T3-L1 (mouse pre-adipocytes), b) BEAS-2B (human normal bronchial epithelial cells), and A549 (human lung epithelial carcinoma) were employed. Cells were seeded in 75 cm^2 cell culture flasks and incubated under appropriate conditions (5% CO_2 at 37 °C and standard humidity) in Dulbecco's modified Eagle's medium DMEM (Sigma, Steinheim, Germany), supplemented with 10% Fetal Bovine Serum FBS (Biochrom, Berlin, Germany) and 1% penicillin-streptomycin (Biochrom, Berlin, Germany). All experiments were run in low passages and cell lines were tested and found free of mycoplasma (MycoAlert® Kit, Promega).

2.5.2. Cell viability assay

To investigate the potential cytotoxic effects of the newly synthesized materials (ligands, cadmium compounds and/or selected chelators), all cell lines, i.e. 3T3-L1 fibroblasts, BEAS-2B and A549 cells were seeded in 96-multi-well plates (2500 cells/well), and treated with the title materials for 24 h in DMEM. Cell viability was assessed by quantifying the ATP present. The amount of ATP is directly proportional to the number of cells present in culture (Promega Corporation, WI, USA). Briefly, the working reagent is added to the cell culture, according to manufacturer instructions (volumetric reagent/supernatant ratio 1:1), without removing the supernatant, as described elsewhere [25]. The luminescence signal intensity, produced by the luciferase reaction, is determined using a Glomax 96 microplate luminometer (Promega Corporation, WI, USA). Cell viability results were also validated via Trypan blue assay.

2.5.3. Cell migration assay

To further investigate the potential cytotoxic profile of the newly-synthesized materials, a cell migration assay was run. The potential inhibition of the endogenous motility of 3T3-L1 pre-adipocytes was evaluated using an in vitro scratch assay. In this regard, cells were seeded in 35 mm cell culture dishes in DMEM and allowed to grow until 70–80% confluency had been achieved. Then, a scratch in the monolayer over the entire diameter of each culture dish was made using a sterile pipette tip (100 μL) and cells were incubated in the culture medium in the presence of a final concentration of 10 μM of the title cadmium compounds. Cells were visualized using an Axio Observer Z1 microscope, with a 10× phase contrast (Carl Zeiss, GmbH Lena, Germany). Images were captured, using an AxioCamHc camera, at two distinct time points 24 and 48 h after the scratch had been made.

2.5.4. Cell morphology

Potential cytotoxic effects, in the presence of the materials tested, were also investigated with respect to cell morphology. To that end, both cell types were regularly examined with respect to shape, appearance, color, confluency, etc., to further confirm any aberration from healthy status. Cells were visualized using an Axio Observer Z1 microscope, with a 10× phase contrast (Carl Zeiss, GmbH Lena, Germany). Images were captured, using an AxioCamHc camera, at several time points (prior and post treatment).

2.5.5. Apoptosis assay

To investigate whether the observed Cd(II)-induced cell death is mediated by a caspase-dependent apoptosis pathway, a Caspase-Glo® 3/7 assay (Promega, USA) was run according to manufacturer instructions. Specifically, 3T3-L1 cells were seeded in appropriate white-walled 96-well plates. Cells were exposed to cadmium compounds at 10, 100 and 1000 μM for 24 h. Caspase-Glo® 3/7 reagent was added to each well (50 μL) and incubated for 2 h at room temperature. Triton X 100 solution (0.05%) was used as a positive control of the assay and untreated cells were considered as negative control. The luminescence of each sample was measured on a GloMax® 96 Microplate Luminometer (Promega Corporation, WI USA). Results were expressed in relative luminescence units (RLU).

2.5.6. Statistical analysis

The data were presented as average and standard error mean (SEM) values of triplicate sets of independent measurements. Mean survival rates and SEMs were calculated for each group. Absolute survival rates were calculated for each control group and one way analysis of variance (ANOVA) was performed for all pair comparisons, followed by post hoc analyses (Tukey). EC_{50} values were also calculated using GraphPad Prism 5 software. Degrees of significance were assessed by three different rating values: $^*p < 0.05$ (significant), $^{**}p < 0.01$ (highly significant) and $^{***}p < 0.001$ (extremely significant) or non-significant ($p > 0.05$).

3. Results

3.1. Synthesis

The synthesis of compounds **1–3** took place in H_2O, whereas compound **4** was synthesized and isolated from a mixture of solvents H_2O-CH_3OH (2:1). All experimental procedures were carried out with simple, commercially available reagents for **1** and **4**, at room temperature or under hydrothermal conditions for **2** and **3**.

Specifically, the reaction between $Cd(NO_3)_2{\cdot}4H_2O$ and α-hydroxy isobutyric acid ($HIBAH_2$) (ratio 1:2) proceeded in water at final pH 5, achieved upon addition of aqueous potassium hydroxide (0.1 N). Addition of cold ethanol to the reaction mixture every 3 days, led to the isolation of colorless crystalline polymeric binary compound **1**. The stoichiometric reaction is shown below (Reaction 1):

$$n\,Cd(NO_3)_2 + 2n\,C_4H_8O_3 + 2n\,KOH \xrightarrow[pH\ 5]{} [Cd(C_4H_7O_3)_2]_n + 2n\,KNO_3 + 2n\,H_2O \quad \text{(Reaction 1)}$$

In the case of **2**, hydrothermal synthesis of a mixture of $Cd(NO_3)_2{\cdot}4H_2O$ and α-hydroxy isobutyric acid ($HIBAH_2$) (ratio 1:2), upon addition of a quantity of an aqueous solution of sodium hydroxide (0.1 N NaOH) (final pH value 5) and subsequent slow evaporation of the resulting solution at room temperature, led to the isolation of the non-polymeric binary colorless crystalline compound **2**, in line with the reaction that follows (Reaction 2):

$$Cd(NO_3)_2 + 2\,C_4H_8O_3 + 2\,NaOH \xrightarrow[pH\ 5]{} [Cd(C_4H_7O_3)_2(H_2O)_2] + 2\,NaNO_3 \quad \text{(Reaction 2)}$$

An analogous reaction (hydrothermal synthesis) between $Cd(NO_3)_2{\cdot}4H_2O$, α-hydroxy isobutyric acid ($HIBAH_2$) and 2,2′-bipyridine (ratio 1:2:1), upon addition of 0.1 N NaOH to a final pH value > 8,

followed by slow evaporation of the reaction mixture, at room temperature, resulted in the isolation of a yellowish crystalline ternary material **3**, according to the following stoichiometric reaction (Reaction 3):

$$2n\ Cd(NO_3)_2 + 2n\ C_4H_8O_3 + 2n\ C_{10}H_8N_2 + 2n\ NaOH + nH_2O \xrightarrow[pH>8]{} [\{Cd_2(C_4H_7O_3)_2(C_{10}H_8N_2)_2(H_2O)_2\}(NO_3)_2]_n \cdot nH_2O + 2n\ NaNO_3$$

(Reaction 3)

In a similar procedure, the reaction between $Cd(NO_3)_2{\cdot}4H_2O$, α-hydroxy isobutyric acid ($HIBAH_2$) and 1,10-phenanthroline (ratio: 1:2:1) in a mixture of solvents H_2O-CH_3OH at room temperature, upon addition of aqueous ammonia (0.1 N) at pH value > 8 and slow evaporation of the emerging solution, led to the formation of the crystalline ternary system **4**, according to the stoichiometric (Reaction 4) that follows:

$$2n\ Cd(NO_3)_2 + 2n\ C_4H_8O_3 + 2n\ C_{12}H_8N_2 + 4n\ H_2O + 2n\ NH_3 \xrightarrow[pH>8]{H_2O/CH_3OH} [\{Cd_2(C_4H_7O_3)_2(C_{12}H_8N_2)_2(H_2O)_2\}(NO_3)_2]_n \cdot 2nH_2O + 2n\ NH_4NO_3$$

(Reaction 4)

Compounds **1–4** were all recovered in a crystalline form. Elemental analysis, FT-IR, and NMR spectroscopy confirmed the X-ray Crystallography results. The new compounds **1–4** are stable in the air for long periods of time.

3.2. Transformation chemistry

The close relationship between compounds **1** and **2** led to an inquiry of the transformation of the polymeric compound to the monomeric compound with the same Cd(II):$HIBAH_2$ molecular stoichiometry. In that respect, hydrothermal treatment of compound **1** in aqueous solution led to the ultimate isolation of crystalline material, which was identified by FT-IR and X-ray crystallography as authentic compound **2**. The stoichiometric reaction of the transformation is shown below:

$$\underset{1}{[Cd(C_4H_7O_3)_2]_n} + 2n\ H_2O \xrightarrow[160\ ^oC,\ 72\ h]{\Delta} \underset{2}{n\ [Cd(C_4H_7O_3)_2(H_2O)_2]}$$

3.3. Description of X-ray crystallographic structures of complexes *1–4*

The X-ray crystal structures of **1–4** show discrete solid-state lattices. The Diamond plots of the crystal structures of the compounds are given in Fig. 1A–D, respectively. Selected bond distances and angles are shown in Table S1.

Compound **1**, $\mathbf{[Cd(C_4H_7O_3)_2]_n}$, crystallizes in the monoclinic space group system $P2_1/c$. The compound is a coordination polymer. The repeating unit of **1** is a mononuclear assembly, formulated by one Cd(II) ion and two α-hydroxy isobutyrato ($HIBAH^-$) ligands. The polymerization of the repeating unit leads to the formation of **1** (Fig. 1A). In the crystalline lattice, one Cd(II) metal center is bound to four singly deprotonated α-hydroxy isobutyric acid ligands through two different modes. Specifically, two of the ligands are coordinated to Cd(II) center through the alcoholic O and one carboxylic O^- moiety (O(1)″, O(1)‴, O(3)″, O(3)‴). The other two $[HIBAH]^-$ ligands are coordinated to Cd(II) ion in a monodentate manner, through the one O^- anchor of the deprotonated carboxylato group (O(2), O(2)′). As a consequence, the Cd(II) center is six-coordinate, with an octahedral geometry around it. The polymer expands into a 2D lattice parallel to the crystallographic b0c plane. One intermolecular hydrogen bonding interaction contributes to the assembled lattice as the alcoholic moiety of one ligand interacts with the carboxylic O(1) anchor of a neighboring ligand.

Compound **2**, $[Cd(C_4H_7O_3)_2(H_2O)_2]$, is a non-polymeric crystalline binary material. It crystallizes in the monoclinic space group C2/c. The

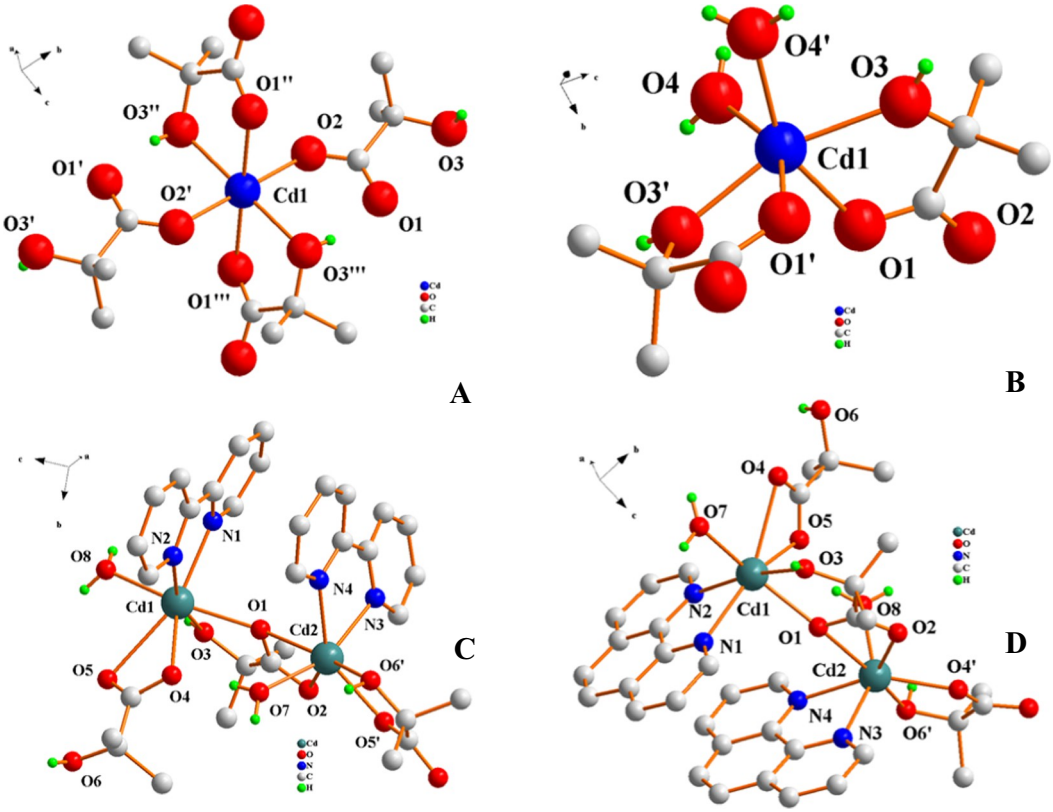

Fig. 1. Diamond plot of complex assemblies in (**A**) $[Cd(C_4H_7O_3)_2]_n$ (**1**), (**B**) $[Cd(C_4H_7O_3)_2(H_2O)_2]$ (**2**), (**C**) $[\{Cd_2(C_4H_7O_3)_2(C_{10}H_8N_2)_2(H_2O)_2\}(NO_3)_2]_n{\cdot}nH_2O$ (**3**), and (**D**) $[\{Cd_2(C_4H_7O_3)_2(C_{12}H_8N_2)_2(H_2O)_2\}(NO_3)_2]_n{\cdot}2nH_2O$ (**4**).

asymmetric unit of **2** contains one cadmium metal center Cd(II), two α-hydroxy isobutyrato $[HIBAH]^-$ anions and two water molecules. The central Cd(II) ion is six-coordinate (Fig. 1B) with an octahedral geometry around it. Specifically, Cd(II) is bound to two singly deprotonated α-hydroxy isobutyric acid ligands in a bidentate mode, through the O-carboxylato and the O-alcoholic terminal of each ligand (O(1), O(3), O(1)′, O(3)′). The other two coordination sites are occupied by the O(4) and O(4)′ atoms of two water molecules. Strong hydrogen bonding interactions emerge as the alcoholic O(3) group of one ligand is interacting with the non-coordinated carboxylic O(2) moiety of a neighboring ligand. Both water molecules also form hydrogen bonds, interacting with two carboxylic O(1) oxygen atoms of two different neighboring ligands (vide infra) (Table S2). All of these intermolecular interactions finally form a 1D lattice, with chains parallel to the *a* crystallographic axis.

Compound **3** is a 1D coordination polymer. It crystallizes in the monoclinic space group $P2_1/c$. Its dinuclear repeating unit consists of two Cd(II) metal centers, two α-hydroxy isobutyrate $[HIBAH]^-$ ions, two 2,2′-bipy and two coordinated water molecules (Fig. 1C). Moreover, two NO_3^- ions (counter ions) and two solvent H_2O molecules per monomer are present in the lattice. Polymerization of the repeating unit leads to the formation of the polymeric crystalline material **3**. The asymmetric unit emerges from two individual polymeric chains with slight differences between them. In the molecular structure, two similar moieties of O-bridged coordinated Cd(II) ions dominate their coordination sphere. Specifically, each Cd(II) metal center is seven-coordinate, with a pentagonal bipyramidal geometry around it. The coordination environment around each Cd center is nearly the same. To that end, Cd(1) is coordinated to two singly deprotonated α-hydroxy isobutyrato $[HIBAH]^-$ ligands in two different modes. One of the $[HIBAH]^-$ ligands is bound to Cd(II) through the two O terminals (O(4), O(5)) of the deprotonated carboxylic acid group. Coordination with the second α-hydroxy isobutyrato ligand takes place through the O^- anchor of the protonated alcoholic (O(3)) and the O^- atom of the deprotonated carboxylic acid group (O(1)). The coordination sphere of Cd(II) is completed with a 2,2′-bipy molecule through its 2 N terminals (*N*(1), N(2)) and a molecule of water (O(8)). Cd(1) is bridged with an adjacent Cd(2) ion through an O atom of the carboxylate moiety of their common singly deprotonated $[HIBAH]^-$ ligand. The chains formed in the arising lattice are also reinforced by π-π interactions between 2,2′-bipy molecules in the same chain (the closest being nearly 3.68 Å). The emerging 1D polymeric lattice encompasses chains parallel to the *c* crystallographic axis.

Strong hydrogen bonding interactions arise as a) O(8) and O(15) oxygen atoms, coordinated to Cd(1) and Cd(4) cations, respectively, belonging to two different chains, and b) the solvent (O(17) and O(18)) water molecules, interact with the oxygen atoms of the nitrate counter anions and the remaining oxygen atoms of the ligands. Intermolecular hydrogen bonding interactions are also present as the alcoholic groups O(3) and O(11) interact with the lattice water molecules O(17) and O(18), respectively. These intermolecular interactions form a strong net and lead to the formation of a final 3D lattice.

Complex **4** is also a 1D coordination polymer. The complex crystallizes in the monoclinic space group $P2_1/c$. The dinuclear repeating unit of the polymer is comprised of two Cd(II) metal ions, two $[HIBAH]^-$ ligands, two phen molecules and two H_2O molecules (Fig. 1D). Lattice water molecules and nitrate ions are also present in the lattice, acting as counter ions. The polymeric ternary material **4** is the result of the polymerization of the repeating unit. Similar to **3**, compound **4** also consists of two identically coordinated Cd(II) metal ions bridged through an O atom of a common $[HIBAH]^-$ ligand. Each cadmium center of the dinuclear moiety Cd-O-Cd is seven-coordinate, giving rise to a pentagonal bipyramidal geometry. Specifically, Cd(1) is coordinated to two singly deprotonated α-hydroxy isobutyrato ligands bound through two different modes. Coordination of one of them to Cd(II) takes place through the oxygen atoms (O(4), O(5)) of the deprotonated carboxylic acid group, whereas coordination with the second $[HIBAH]^-$ ligand occurs through the alcoholic O (O(3)) and one carboxylic O (O(1)) terminal. Two N-anchors (*N*(1), N(2)) of a phen molecule cover two coordination sites around a Cd(II) ion. The coordination environment around the cadmium metal center is completed with an O(7) atom of a water molecule. An O carboxylic terminal (O(1)) of a common $[HIBAH]^-$ ligand functions as a monoatomic bridge between the adjacent Cd(1) and Cd(2) metal centers, which are also O^- bridged, with other neighboring Cd-O-Cd moieties on a similar mode.

Interligand hydrogen bonding interactions are present between the coordinated and lattice water molecules, and the nitrate counter ions and oxygen atoms of $[HIBAH]^-$ ligands, as they hold them together, thereby promoting stability of the arising chains. In these interactions, all carboxylato oxygen atoms and alcoholic groups are involved. The chains formed are also enhanced as π-π interactions between phen molecules in the same chain (the closest being nearly 3.57 Å) result in a preliminary 1D polymer arrangement, with the chains being parallel to the *c* crystallographic axis. Finally, π-π interactions between phen ligands of neighboring chains (the closest being nearly 3.49 Å) result in the formation of a 2D coordination polymer, with planes being parallel to the b0c crystallographic plane.

3.4. FT-IR spectroscopy

The FT-Infrared spectra of compounds **1–4** exhibit vibrationally active carboxylates. Antisymmetric and symmetric vibrations of the specific groups were observed in all spectra, with antisymmetric stretching vibrations $\nu_{as}(COO^-)$ emerging at 1580 cm^{-1} for **1**, 1630 cm^{-1} for **2**, 1590 cm^{-1} for **3**, and 1583 cm^{-1} for **4**, and symmetric stretching vibrations of the same groups arising in the range 1450–1360 cm^{-1}, 1480–1350 cm^{-1}, 1440–1360 cm^{-1}, and 1419–1303 cm^{-1}, respectively. Shifts of the frequencies of the observed carbonyl vibrations to lower values in comparison to the corresponding vibrations in free α-hydroxy isobutyric acid ($HIBAH_2$) were observed, attesting to changes in the vibration status of the ligand binding to the Cd(II) ion. A similar behavior had been previously observed in analogous compounds of divalent metal ions bound to deprotonated α-hydroxycarboxylato ligands [26,27].

3.5. Solution NMR spectroscopy

The solution ^{13}C NMR spectra of freshly prepared compounds **1** and **2** were recorded in D_2O. The spectra of **1–4** (Fig. 2A–D) exhibit a a) resonance at 26.7 ppm for **1** and **2**, 27.0 ppm for **3** and 26.6 ppm for **4**, attributed to the $[HIBAH]^-$ methyl carbons, b) a resonance at 73.6 ppm for **1–4**, attributed to the quaternary carbon, c) resonances in the range 123.6–149.5 ppm attributed to the presence of aromatic carbons in the 2,2′-bipy ligand for **3**, and in the range 125.1–149.5 ppm attributed to the presence of aromatic carbons of the phen ligand in **4**, and d) a resonance at 184.0 ppm for **1–2**, 184.4 ppm for **3**, and 183.6 ppm for **4**, in agreement with the presence of the carboxylato carbon of the $[HIBAH]^-$ ligand bound to the Cd(II) ion. The above observations were consistent with the structure of the respective compounds determined by X-ray crystallography.

The ^1H NMR spectra of **1–4** in D_2O showed several peaks. The spectra of **1–4** (Fig. S1A–D) exhibit a resonance at 1.2 ppm, consistent with the presence of the methyl protons ($[HIBAH]^-$ group). The resonances in the range 7.5–8.3 ppm for **3** and 7.8–8.8 ppm for **4** could be attributed to the presence of aromatic protons in the 2,2′-bipy and the 1,10-phen Cd(II)-bound ligands, respectively.

3.6. ESI-MS results

The aqueous behavior of **1–4**, upon dissolution of the respective compounds in water, was revealed through ESI-MS measurements run in positive mode. The species identified were the following: for **1**,

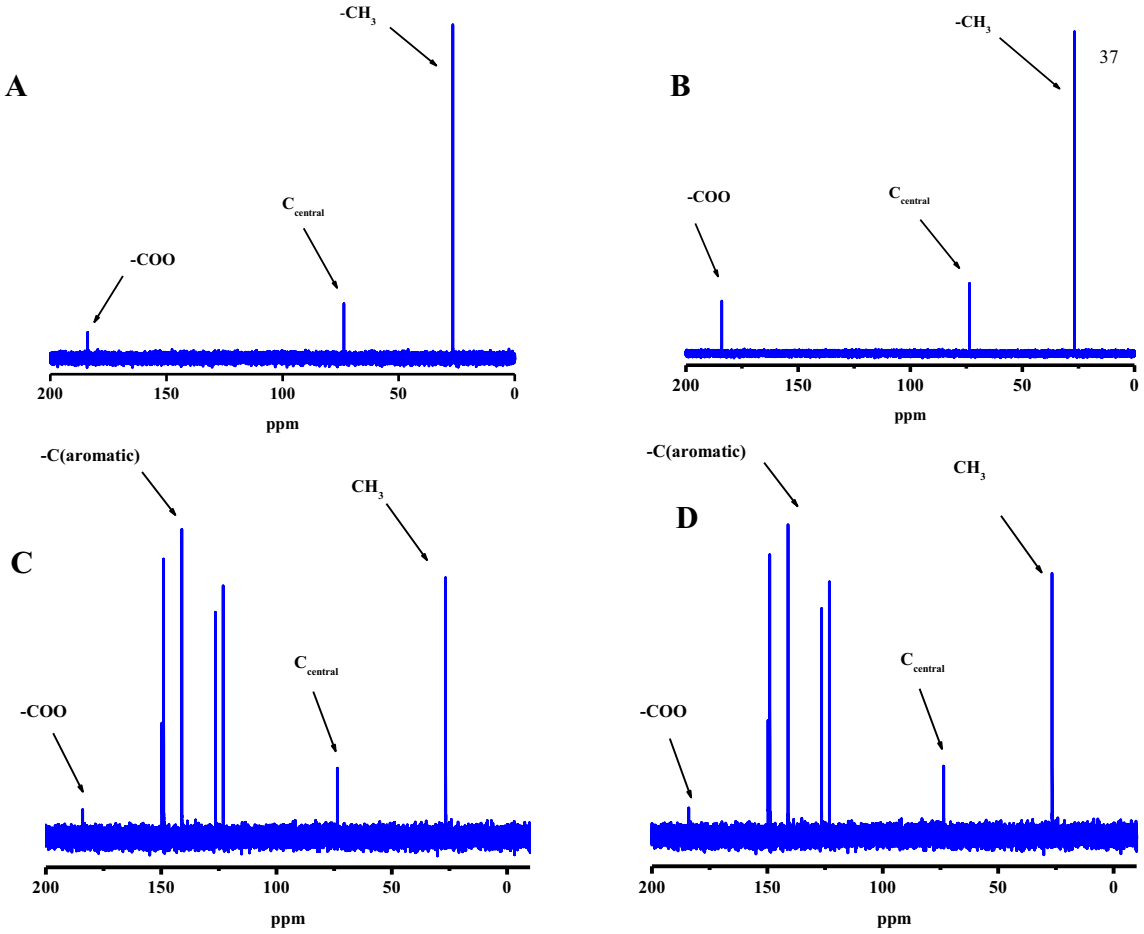

Fig. 2. ^{13}C NMR spectra of **A**) **1**, **B**) **2**, **C**) **3**, and **D**) **4**.

M_1 = [Cd(L)$_2$], (m/z = 320.9890, z = 1, [M_1H]$^+$) (Fig. S2B); for **2**, M_1 = [Cd(L)$_2$], (m/z = 320.9890, z = 1, [M_1H]$^+$), M_2 = [Cd(L)$_2$(H$_2$O)], (m/z = 338.9890, z = 1, [M_2H]$^+$), and M_3 = [Cd(L)$_2$(H$_2$O)$_2$], (m/z = 397.0108, z = 1, [M_3H]$^+$) (Fig. S3B); for **3**, M_1 = [Cd(L)(2,2′-bipy)], (m/z = 373.0099, z = 1, [M_1H]$^+$) (Fig. S4B); and for **4** M_1 = [Cd(L)(1,10-phen)], (m/z = 397.0097, z = 1, [M_1H]$^+$) and M_2 = [Cd(L)$_2$(1,10-phen)(H$_2$O)$_2$], (m/z = 577.0871, z = 1, [M_1K]$^+$) (Fig. S5B).

3.7. Thermal studies

The thermal decomposition of representative Cd(II) compounds **1** and **3** was investigated under an oxygen atmosphere. Compound **1** is stable up to 250 °C (Fig. S6A), whereas compound **3** appears to behave differently from the beginning of the combustion process (Fig. S6B), with a weight loss being observed from 25 °C until 200 °C due to the presence of coordinated and lattice water. Subsequently, a continuous weight loss is observed between 250 °C and 462 °C for **1**, and 200 °C to 432 °C for **3**, in line with the decomposition of the organic part of the compound. In these stages, no clear plateaus are reached for **1** and **3**, suggesting that the derived products are unstable and decompose further. There is no further weight loss beyond 462 °C for **1** and 432 °C for **3**, with CdO being the final product beyond that temperature. The total weight loss is 60.0% (calc. 59.7%), in agreement with the following tentative reactivity in the case of **1**:

$$[Cd(C_4H_7O_3)_2]_n + 9n\ O_2 \longrightarrow n\ CdO + 8n\ CO_2 + 7n\ H_2O$$

In the case of compound **3**, the total weight loss is 80.3% (calc. 79.6%), in line with the following reactivity:

$$[\{Cd_2(C_4H_7O_3)_2(C_{10}H_8N_2)_2(H_2O)_2\}(NO_3)_2]_n \cdot nH_2O + 61/2n\ O_2 \longrightarrow 2n\ CdO + 28n\ CO_2 + 18n\ H_2O + 3n\ N_2$$

3.8. Cytotoxicity results

3.8.1. Cadmium compound toxicity in 3T3-L1 cells

Prior to evaluating compound toxicity, the (a)toxic profile of the employed ligand (HIBAH$_2$) was assessed. The results show that the specific ligand does not affect cell survival under the employed experimental conditions (Fig. 3), thereby suggesting that any toxicity detected is due to cadmium metal ion (in the currently complexed form). In an analogous fashion, work on the other two cell lines (BEAS-2B and A549) showed that the ligand is atoxic over the same concentration range (1–500 μM) (data not shown). Subsequently, the potential cytotoxic effects of the newly synthesized cadmium compounds **1–4** were investigated. 3T3-L1 cells were exposed to cadmium compounds at several concentrations (1–500 μM) for 24 h. Fig. 4A–D shows that cell survival is affected at concentrations higher or equal than 10 μM in almost all cases. Compound **1** is completely atoxic at 1 and 10 μM (116.0 ± 6.4 and 105.0 ± 5.6%, respectively ($p > 0.05$)). Cell survival is significantly reduced at 100 and 500 μM (38.7 ± 5.0 and 0.6 ± 0.1% ($p < 0.001$), respectively). By the same token, survival amounts to 103.2 ± 7.0, 83.5 ± 1.3, 11.3 ± 0.7 and 0.4 ± 0.1% at concentrations 1, 10, 100 and 500 μM, respectively, in the case of compound **2**. When cells are treated with compound **3**, cell survival amounts to 109.2 ± 2.3, 98.4 ± 6.7, 18.5 ± 2.3, and 1.1 ± 0.2% for the same concentration range, whereas for compound **4** cell survival

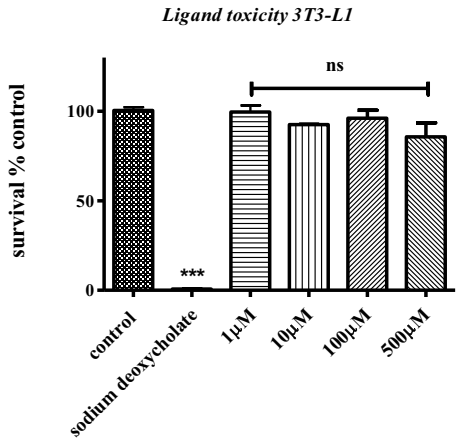

Fig. 3. Percent change of cell survival in 3T3-L1, following treatment with various concentrations (1–500 μM) of 2-hydroxy isobutyric acid for 24 h. Sodium deoxycholate was used as a positive control. Values represent the mean value of several ($n = 3$) independent experiments. Vertical bars represent SEMs. $*p < 0.05$ (significant), $**p < 0.01$ (highly significant) and $***p < 0.001$ (extremely significant) or non-significant ($p > 0.05$).

emerged at 107.6 ± 5.3, 88.9 ± 2.8, 9.1 ± 1.8, and 2.1 ± 0.7%. The EC_{50} values are presented in Table 2.

3.8.2. Cadmium compound toxicity in BEAS-2B cells

Cadmium compound toxicity was also tested in BEAS-2B cell cultures. To this end, cells were treated with **1**–**4** at various concentrations (1–500 μM) for 24 h. The results show that **1** affects cell survival in a concentration-dependent manner. More specifically, cell survival amounts to 105.7 ± 5.3 and 104.7 ± 3.6% at 1 and 10 μM, respectively ($p > 0.05$) (Fig. 5A). When cells are treated with 100 μM of compound **1**, cell survival is reduced by ~20% and complete abolishment of cell viability is observed at 500 μM ($p < 0.001$) (Fig. 5A). In the case of **2**, cell survival is not affected at concentrations 1 and 10 μM (104.1 ± 2.7 and 107.5 ± 1.8%, respectively ($p > 0.05$)). Cell exposure at 100 μM causes significant reduction of cell viability (16.0 ± 0.8%), whereas cell survival is totally reduced ($p < 0.001$) at 500 μM (Fig. 5B). In the case of compound **3**, cell survival follows a concentration-dependent manner as well. In more detail, cell survival amounts to 100.5 ± 2.4, 87.0 ± 4.1, 29.4 ± 4.5 and 2.4 ± 0.1% at 1, 10, 100 and 500 μM, respectively (Fig. 5C). Compound **4** appears to be toxic even at low concentrations (1 and 10 μM). More specifically, cell survival amounts to 93.7 ± 8.1, 71.9 ± 5.1, 12.7 ± 1.0 and 3.2 ± 0.1% at 1, 10, 100 and 500 μM, respectively (Fig. 5D). The EC_{50} values are presented in Table 2.

Table 2
EC_{50} values of compounds of **1**–**4** in the three 3T3-L1, BEAS-2B, and A549 cell lines.

Compound	1	2	3	4
EC_{50} value (μM) 3T3-L1	67	25.7	38.3	23.4
EC_{50} value (μM) BEAS-2B	300	70.9	52.0	22.6
EC_{50} value (μM) A549	273	131.5	63.0	15.6

3.8.3. Cadmium compound toxicity in A549 cells

Having assessed cell toxicity profile in BEAS-2B cell cultures, cell survival was also tested in A549 cells (presenting the comparative case of physiological vs cancer cell cultures). In the presence of compound **1**, cell survival amounts to 98.0 ± 1.6, 99.4 ± 0.7, and 93.3 ± 2.3% for

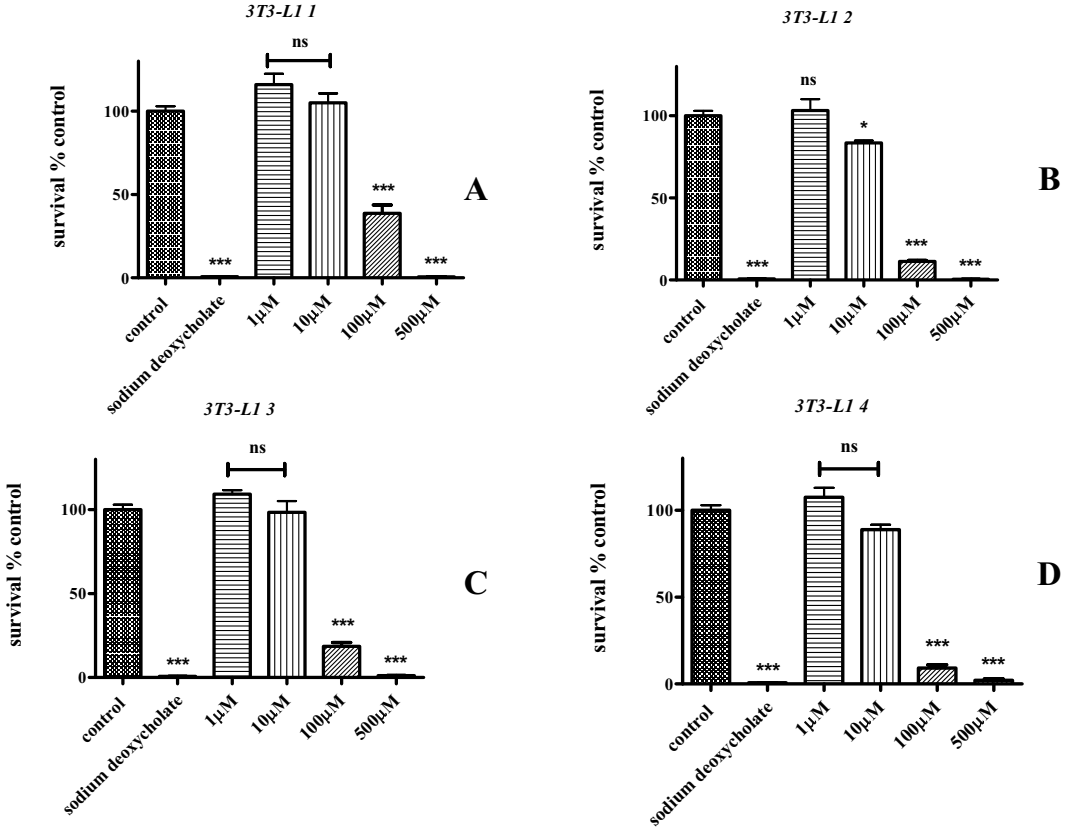

Fig. 4. Percent change of cell survival in 3T3-L1, following treatment with various concentrations (1–500 μM) of **A**) **1**, **B**) **2**, **C**) **3**, and **D**) **4** for 24 h. Sodium deoxycholate was used as a positive control. Values represent the mean value of several ($n = 3$) independent experiments. Vertical bars represent SEMs. $*p < 0.05$ (significant), $**p < 0.01$ (highly significant) and $***p < 0.001$ (extremely significant) or non-significant ($p > 0.05$).

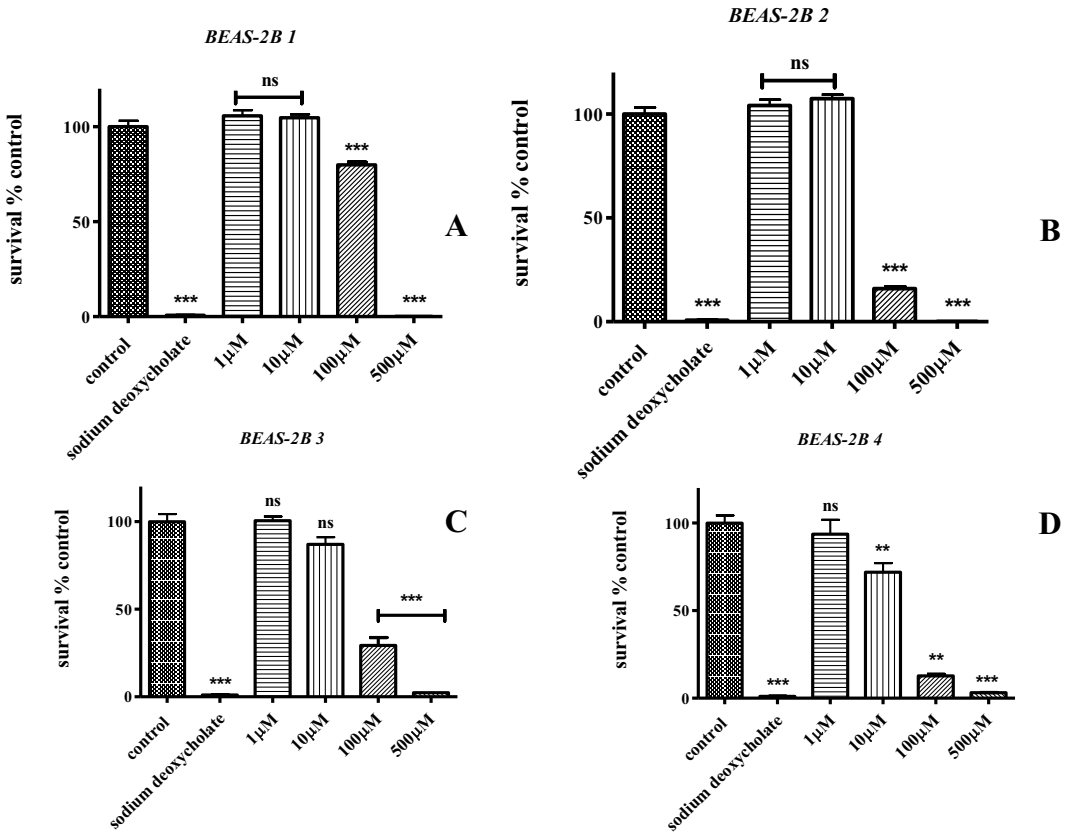

Fig. 5. Percent change of cell survival in BEAS-2B, following treatment with various concentrations (1–500 μM) of **A**) **1**, **B**) **2**, **C**) **3**, and **D**) **4** for 24 h. Sodium deoxycholate was used as a positive control. Values represent the mean value of several (n = 3) independent experiments. Vertical bars represent SEMs. *p < 0.05 (significant), **p < 0.01 (highly significant) and ***p < 0.001 (extremely significant) or non-significant (p > 0.05).

concentrations 1, 10, and 100 μM ($p > 0.05$). Cell survival is significantly reduced when cells are treated at high concentrations (23.1 ± 0.7%, 500 μM) ($p < 0.001$) (Fig. 6A). Compound **2** seems to follow a cell survival pattern identical to compound **1**. More specifically, cell survival is not affected at concentrations 1 and 10 μM (105.5 ± 1.7 and 107.7 ± 0.8%, respectively (p > 0.05)). Cell survival is slightly reduced (by ~20%), when cells are treated with 100 μM of **2**, whereas at 500 μM, cell survival amounts to 13.1 ± 0.3 (p < 0.001) (Fig. 6B). Cell survival in the presence of compound **3** amounts to 108.0 ± 5.0, 105.6 ± 7.6, 42.8 ± 0.5%, whereas for compound **4**, cell survival amounts to 98.2 ± 3.1, 56.7 ± 4.8, 33.0 ± 1.4 and 26.1 ± 0.5% for the same concentration range (Fig. 6C–D). The EC_{50} values are presented in Table 2.

3.8.4. Cell migration results in 3T3-L1 cells

To assess cell migration effect(s) of cadmium compounds, **1** and **2** were selected for further investigation. The selection was based on solubility-bioavailability criteria (vide infra). To this end, a scratch assay was performed using 3T3-L1 pre-adipocytes. Cells were treated with 10 μM of each compound for 24 and 48 h, respectively (10x 5× magnification). The migration capacity of cells, grown in the presence of only DMEM, was considered as control. As shown in Fig. 7, compound **1** projected a complete abolishment of migration at the concentration tested. In the case of compound **2**, cells also exhibited reduced migration. Similar patterns were obtained after treatment for 48 h (Fig. S7), although it should be pointed out that cell viability is significantly reduced following treatment for longer periods at the same concentration(s) tested.

3.8.5. Caspase 3/7 activity in 3T3-L1 cells

Cell death can be classified, based on cell morphology, as apoptotic, necrotic, necroptotic, autophagic or related to mitosis. In an effort to investigate the potential activation of the apoptotic pathway in the presence of **1** and **2**, an apoptosis assay was performed with respect to caspase 3/7 (known apoptosis biomarker) relative activity in 3T3-L1 cells. For this purpose, cells were treated with either **1** or **2** at distinct concentrations (10, 100, and 1000 μM) for 24 h. Triton X 100 solution (0.05%), which was used as a positive control, projected a 2.6 fold increase in caspase 3/7 relative activity, compared to the control (untreated cells, incubated only in DMEM) (Fig. 8A–B). Compound **1** induced the expression of caspase 3/7 in a concentration-dependent fashion. More specifically, **1** projected a ~2.4 fold increase in caspase 3/7 relative activity at 10 μM, a 1.3 fold increase at 100 μM and 0.53 fold activity at 1000 μM. Caspase 3/7 relative activity amounts to ~3.3 in the case of compound **2** at 10 μM, 1.2 fold increase at 100 μM, and 0.56 fold increase at 1000 μM.

3.8.6. Cytoprotective activity of selected chelators and antioxidants

In the previous section, a comparative assessment toward cytotoxicity took place with respect to normal vs cancer state cells (BEAS-2B vs A459). In view of the arisen results, the potential cytoprotective activity of known antioxidants (N-Acetyl Cysteine, NAC) and chelators (8-hydro-7-iodo-5-sulfonic acid, HO-I-SA) was assessed. Cells were exposed to the aforementioned agents for 1 h and then compounds **1** and **2** were added at a stoichiometric ratio 1:1 at 100 and 500 μM (cell survival decreasing concentrations). Prior to that, it was deemed necessary to investigate whether these agents affect cell survival alone, under the same experimental conditions, thereby allowing for selection of optimum exposure conditions. In so doing, both cell types (BEAS-2B and A459) were treated with either NAC or HO-I-SA for 24 h, at concentrations 100 and 500 μM. The results show that NAC is completely atoxic in all cases (both concentrations and cell types) (Fig. 9A–B). HO-

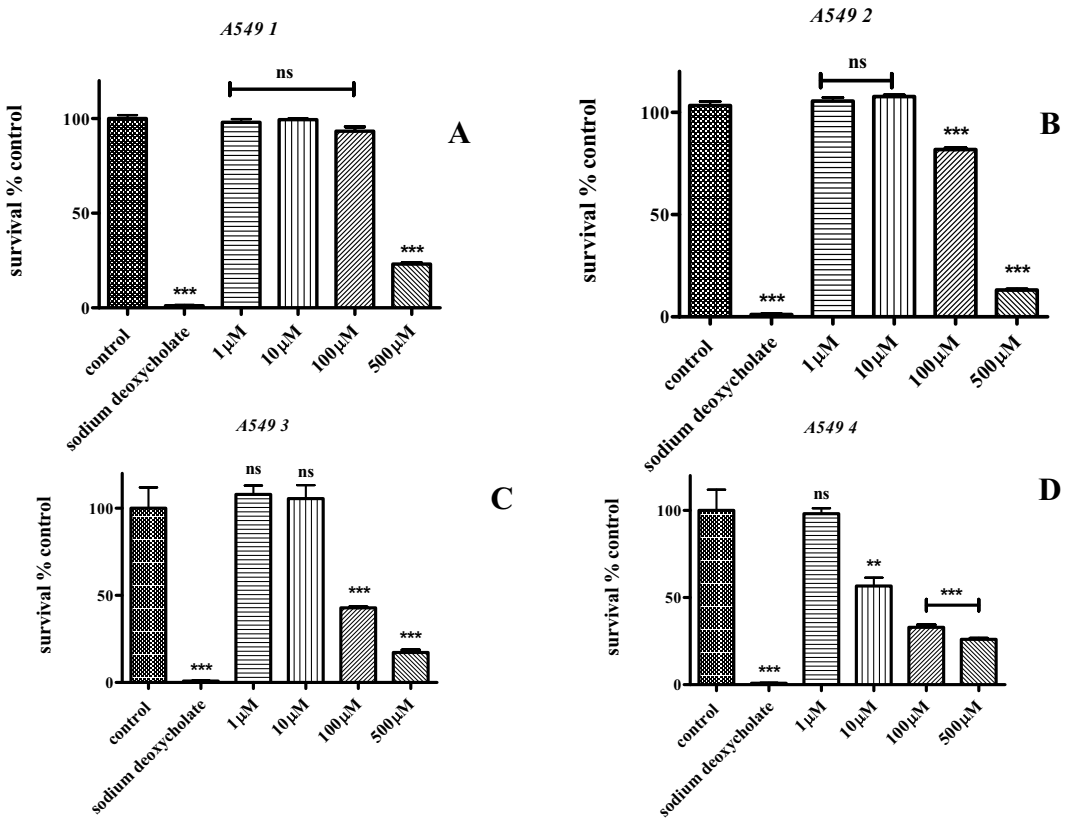

Fig. 6. Percent change of cell survival in A549, following treatment with various concentrations (1–500 μM) of **A**) **1**, **B**) **2**, **C**) **3**, and **D**) **4** for 24 h. Sodium deoxycholate was used as a positive control. Values represent the mean value of several (n = 3) independent experiments. Vertical bars represent SEMs. *p < 0.05 (significant), **p < 0.01 (highly significant) and ***p < 0.001 (extremely significant) or non-significant (p > 0.05).

I-SA appears to be atoxic at 100 μM, whereas at 500 μM cell survival is reduced by ~60% in both cell types ($p < 0.001$) (Fig. 9A–B).

In the case of BEAS-2B cells, when cells are treated with 100 μM, only in the presence of **1** and **2**, cell survival amounts to ~80% for **1** and 16% for **2**, respectively (vide supra). When cells are pre-exposed to HO-I-SA (1:1), cell survival amounts to 63.5% and 78.3%, for **1** and **2**, respectively, tested at the same concentration (100 μM). By the same token, cell survival amounts to 0.2 and 0.1% at 500 μM for **1** and **2**. Pre-

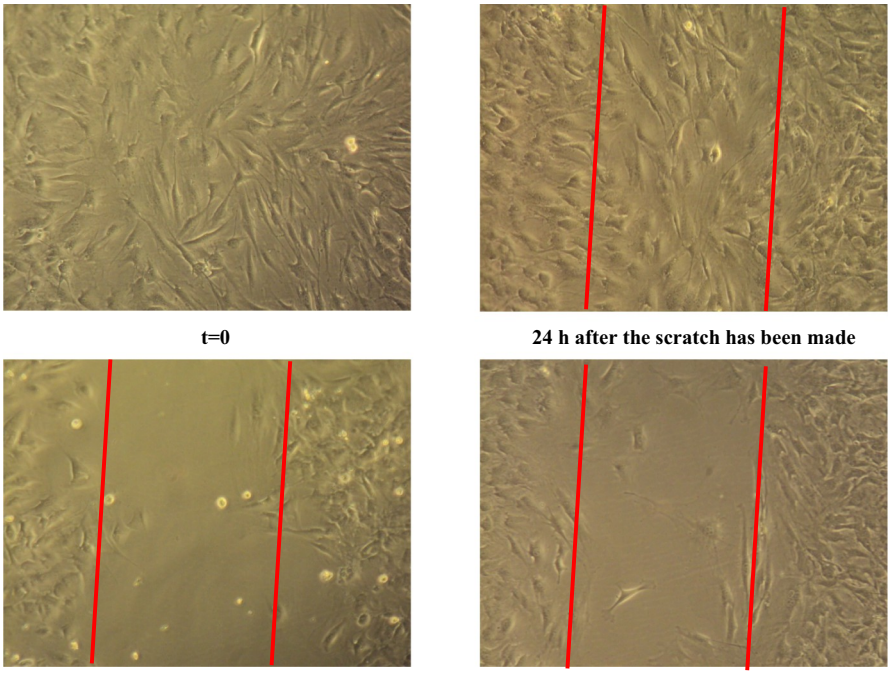

Fig. 7. Cell migration of 3T3-L1 **A**) control ($t = 0$), **B**) control after 24 h. Cells treated with 10 μM of **C**) **1**, and **D**) **2**, using a standard scratch assay.

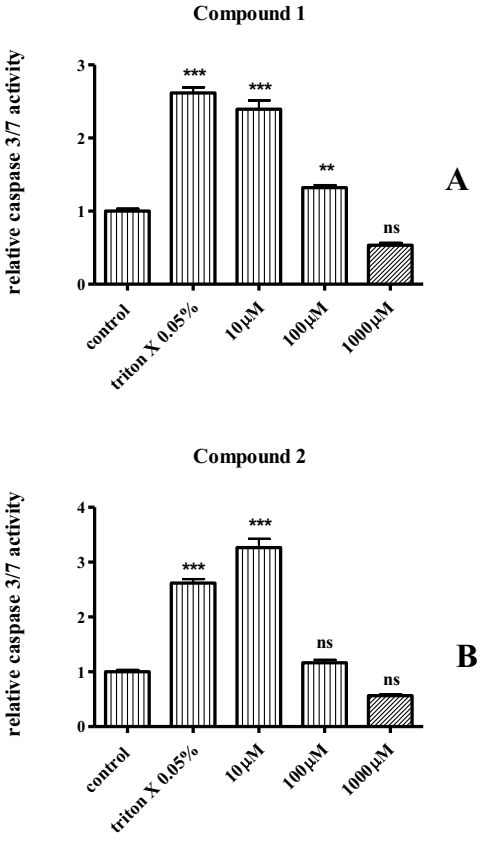

Fig. 8. Relative caspase (3/7) activity in 3T3-L1, following treatment with 10, 100 and 1000 μM of **A**) **1**, and **B**) **2** for 24 h. Values represent the mean value of several (n = 3) independent experiments. Vertical bars represent SEMs. *: $p < 0.05$ vs. control. *$p < 0.05$ (significant), **$p < 0.01$ (highly significant) and ***$p < 0.001$ (extremely significant) or non-significant ($p > 0.05$).

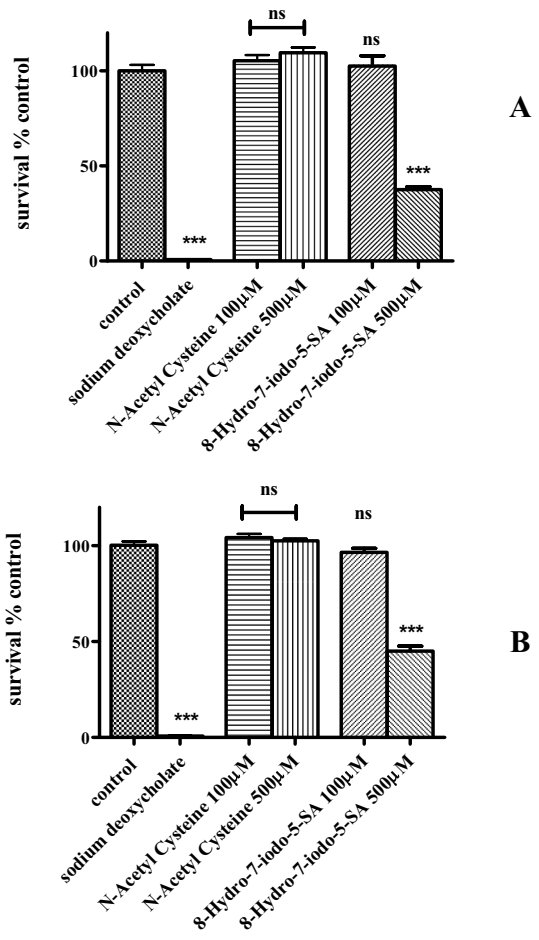

Fig. 9. Percent change of cell survival in **A**) BEAS-2B, and **B**) A549, following treatment with 100 and 500 μM of NAC and HO-I-SA, respectively for 24 h. Sodium deoxycholate was used as a positive control. Values represent the mean value of several (n = 3) independent experiments. Vertical bars represent SEMs. *$p < 0.05$ (significant), **$p < 0.01$ (highly significant) and ***$p < 0.001$ (extremely significant) or non-significant ($p > 0.05$).

exposure with HO-I-SA results in cell survival amounting to 14.7 and 1.1%, respectively. In the case of A549 cells, when cells are treated with 100 μM, cell survival amounts to 93.3% and 81.8% for **1** and **2** alone, respectively. Pre-exposure with HO-I-SA (1:1) results to 80.3% for **1** and 64.3% for **2**. At 500 μM, cell survival amounts to 23.1% and 13.1%, respectively, for **1** and **2** (when employed alone). However, in the presence of HO-I-SA, cell survival rises to 65.8% and 41.3%, respectively (Fig. 10A–B). In a similar effort, the potential cytoprotective effect of NAC was also assessed. As shown in Fig. 10C, NAC induces a slight, insignificant protective effect for both compounds tested on BEAS-2B cells. The same results were obtained in the case of A549 (data not shown).

4. Discussion

4.1. The binary and ternary chemistry of Cd(II) with hydroxycarboxylic moieties

Cadmium is an established environmental contaminant, influencing dramatically animal, plant and human survival [4,11,14,15,17,28]. Exertion of its biotoxicity is strongly correlated to its interaction(s) with organic cellular substrates. To that end, coordination of Cd(II) with physiological and/or physiologically relevant organic chelators leads to potentially more soluble forms, further enhancing its bioavailability and promotion of toxic manifestations [26,27]. Delving into the investigation of structural-biological interactions of Cd(II) with low molecular mass biogenic molecules, such as α-hydroxycarboxylic acids [19], presents a unique opportunity for development of the relevant synthetic chemistry involving α-hydroxy isobutyric acid ($HIBAH_2$) [12,26,27,29]. The herein reported synthetic chemistry in aqueous media, under pH-specific conditions and molecular stoichiometries afforded crystalline materials **1–4**, further characterized by analytical, spectroscopic and crystallographic methods. Two of them were binary species, with the remainder being ternary species encompassing N,N'-aromatic chelators. The importance of pH and molecular stoichiometry in achieving the successful synthesis and isolation of the aforementioned materials is clearly exemplified through the first two compounds $[Cd(C_4H_7O_3)_2]_n$ (**1**) and $[Cd(C_4H_7O_3)_2(H_2O)_2]$ (**2**), of which **1** was a coordination polymer, with **2** being a non-polymer mononuclear species. Given the striking similarity between the two basic units in **1** and **2**, bearing a Cd(II):ligand ratio 1:2, the possibility of conversion between the discrete and polymeric species arose as a challenge. To that end, under appropriately selected conditions, hydrothermal reactivity led to the conversion of **1** to **2**. The transformation denotes the possibility of polymer **1** dissociating under the employed reaction conditions, thereby giving rise to the discrete molecular species **2**. It's worth noting that under the employed aqueous conditions, dissociation of the polymer generates two vacant sites in the coordination sphere of Cd(II), thereby providing the opportunity for water molecules to bind the metal ion, thus fulfilling its coordination requirements (Scheme 1). The latter features project clear retention of the coordination number of Cd(II) during the transformation process, thereby lending credence to the crystallographic determination of the isolated compounds **1** and **2**, both bearing an octahedral coordination sphere around the central metal ion.

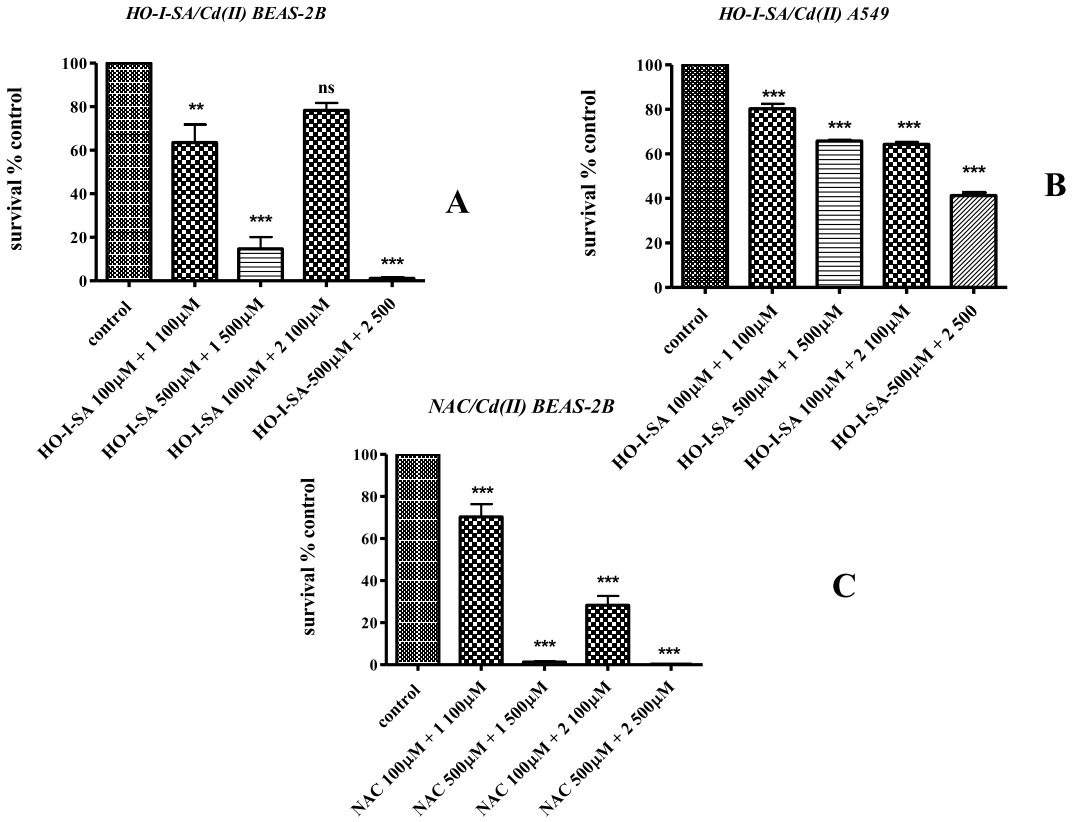

Fig. 10. Percent change of cell survival in **A**) BEAS-2B, and **B**) A549, following treatment with of **1** and **2** (100 and 500 μM) for 24 h, after being exposed to 1:1 stoichiometric ratio of HO-I-SA for 1 h or NAC (**C**) in BEAS-2B. Sodium deoxycholate was used as a positive control. Values represent the mean value of several (n = 3) independent experiments. Vertical bars represent SEMs. *: $p < 0.05$ vs. control. *$p < 0.05$ (significant), **$p < 0.01$ (highly significant) and ***$p < 0.001$ (extremely significant) or non-significant ($p > 0.05$).

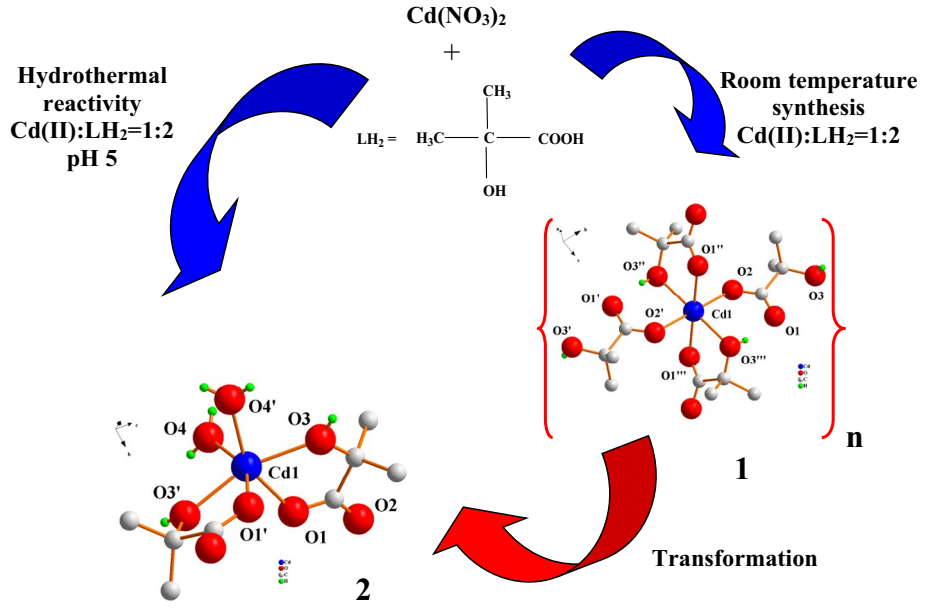

Scheme 1. Synthetic reactivity and transformation involving **1** to **2**.

4.2. Ternary interactions of Cd(II) with HIBAH$_2$ and the presence of N,N′-aromatic donors

Beyond binary interactions with appropriately structured partners in aqueous media, the potential of Cd(II) being involved in ternary interactions with ternary participant targets necessitates that appropriate binders be introduced to the reaction mixture. To that end, N,N'-aromatic chelators 2,2′-bipy and 1,10-phen were introduced and the requisite chemistry was examined under appropriate reaction conditions.

The thus synthetically derived materials were isolated in crystalline form and include compounds

$[\{Cd_2(C_4H_7O_3)_2(C_{10}H_8N_2)_2(H_2O)_2\}(NO_3)_2]_n \cdot nH_2O$ (**3**), and $[\{Cd_2(C_4H_7O_3)_2(C_{12}H_8N_2)_2(H_2O)_2\}(NO_3)_2]_n \cdot 2nH_2O$ (**4**). Both materials are coordination polymers and reveal a dinuclear repeating unit, incorporating the singly deprotonated ($HIBAH^-$) ligand and the aromatic chelators in the basic assembly. In both cases, the Cd(II):LH^-:chelator ratio is 1:1:1. Therefore, the structural formulation of the repeating unit in **3** and **4** is starkly differentiated from that in **1**, thereby reflecting the chelating, bulk and binding properties of the aromatic chelators in the coordination sphere of Cd(II). In such an assembly, the presence of coordinated water molecule in the coordination sphere of Cd(II) signals further chemical reactivity on the fundamental assembly of the polymer and is currently being probed into in the lab. Lattice water molecules, albeit in different numbers in **3** and **4**, signify the contribution of that solvent to the stabilization of the respective lattices through hydrogen bond formation [30]. The spectroscopic and structural changes occurring in the coordination sphere of the Cd(II)-[$HIBAH^-$] binary moiety, upon introduction of the aromatic chelators, project the input of factors influencing the nature of the basic repeating unit of the lattices in **3** and **4**, introducing both bulk, hydrophobicity, and π-π interactions as parameters in the stabilization of the dinuclear assembly. As a result of that, the [$HIBAH^-$] ligand is encountered both as a terminal as well as bridging ligand, bringing two mononuclear Cd(II) assemblies together into one unit, with the aid of the singly deprotonated ligand acting as the connector stabilizing the overall assembly. It is this role of the ($HIBAH^-$) ligand that, due to the introduction of the aromatic N,N′-chelators, necessitates the introduction of water in the coordination sphere of each participating Cd(II) center in the dinuclear assembly, thereby differentiating the repeating unit in **1** from that in **3** and **4**. Both of the assemblies in the ternary materials project a pentagonal bipyramidal geometry around each Cd(II) center in the repeating unit, similar to other ternary cadmium systems with glycolic acid and the N,N′-aromatic chelators 2,2′-bipy and 4,4′-bipy as well [26].

A more extensive physicochemical characterization of **1–4** through elemental analysis, FT-IR, NMR, ESI-MS and TGA techniques in the solid state and solution resulted in well-defined physicochemical correlation profiles for **1–4**, thereby a) lending credence to the emerging species that could engage third partners in a cellular milieu, and b) supporting the observed cytotoxicity of the discrete cadmium species employed in biological experiments. Based on such grounds, in the case of binary compounds **1** and **2**, interesting was the distinct nature of their solution profile, supported by NMR and ESI-MS measurements, thereby presaging observations of their distinct biological profile compared to that projected through crystallographic work. Collectively, the individual and cumulative work on all four species supports the notion of structural speciation in binary or ternary systems, such as those of Cd(II) with [$HIBAH^-$] and the two aromatic chelators, contributing (through their attributes of solubility, bioavailability, bulk, hydrophilicity-hydrophobicity, etc.) to the generation of the cytotoxicity profile for Cd(II), the coordination sphere composition of which appears to bear on its interactions into cellular processes and cell integrity (vide infra).

4.3. The biological profile of cadmium species

As in all cases of exposure to a toxic agent, cadmium toxicity depends on several factors involving route, dose, time, rate, tissue, and the form of the metal ion (speciation) when it comes to metallotoxins [9]. It has been shown that cadmium can affect several biological systems in vitro, in vivo or at the clinical level [31]. In that context, cadmium can impair bone metabolism through vitamin D imbalance. Several studies support the fact that there is a strong correlation between obesity, diabetes and toxic metal ions such as cadmium [32,33]. Wet lab studies indicate that cadmium can influence adipose tissue pathophysiology in many ways, thereby leading to insulin resistance and ultimately diabetes. However, the existing epidemiological data concerning the impact of cadmium exposure on obesity and diabetes are still contradictory and further investigation needs to be carried out. Moreover, cadmium can act as a metalloestrogen, mainly studied in breast and ovarian cancer [34]. Cadmium-induced carcinogenicity in lung remains unclear, based on cohort studies, although there is strong evidence that cadmium acts as a carcinogenic agent in general [35]. It is worth noting that most of the in vitro or in vivo studies employ commercially available forms of cadmium that lack bioavailability or project variable solubility in water. Such forms include cadmium chloride, cadmium sulfate, and cadmium nitrate, or even cadmium oxide and cadmium sulfide. Previous work from our laboratory supported the fact that cadmium projects differential biotoxic behavior with respect to solubility, structure-specificity and thermodynamics of interactions, toward concentration, time, and tissue of the system under investigation [27]. All of the aforementioned were considered as the state of the art of the present study, aiming to assess the biological profile of the title compounds in selective in vitro biological systems, closely linked to representative pathophysiologies (e.g. adipose tissue, lung epithelium). To that end, the specifically employed cell lines (3T3-L1, BEAS-2B, and A549) stand as valuable models to study the impact of such metallotoxins. Initially a cell viability assay was run in an effort to assess the impact of **1–4** on cell survival in all cell lines employed. The results indicate that cell survival decreases in a concentration-dependent manner for all compounds tested. Moreover, the experiments showed that the observed cell death was mediated through the apoptotic pathway in a concentration-dependent fashion, thereby projecting the role of biomarker caspases in the delineation of the emerging behavior of Cd(II) species **1** and **2** (Fig. 8). The EC_{50} values for each compound tested were calculated following a 24 h treatment for each cell line used. The EC_{50} values are plotted in Fig. 11. The overall results suggest that Cd(II) compounds project a distinct toxicity behavior under the employed experimental conditions for the three cell lines. Taking into account the mean survival rates, A549 cells appear to be less vulnerable to Cd(II) toxicity. When considering the structure of the employed compounds and the species appearing in solution, it appears that the cytotoxic potential is enhanced, in line with the structural variability of the complex form(s) of each compound (vide infra).

Compound **1** appears to be less bioavailable compared to **2**, as **2** tends to be more toxic. Compounds **3** and **4** appear to be the most toxic species of all four tested, as they exhibit the lowest EC_{50} values in all three cell lines examined. They are the ones encompassing 2,2′-bipy (**3**) and phen (**4**) and at the structural level they bear double the amount of Cd(II) compared to **1** and **2**. Also worth pointing out is the fact that both **3** and **4** essentially exhibit the same composition, with the only difference being the presence of the two distinctly formulated N,N'-aromatic chelators with the specific bulk they carry. In that sense, their toxicity profile appears to be very similar in both cases as that is also indicated by the EC_{50} diagram (Fig. 11).

Moreover, when cells are exposed to low cadmium concentrations (1 μM), a slight proliferative effect is detected. This observation is in line with literature data supporting the fact that cadmium induces cell proliferation at nM concentrations [16,36]. Further investigation in

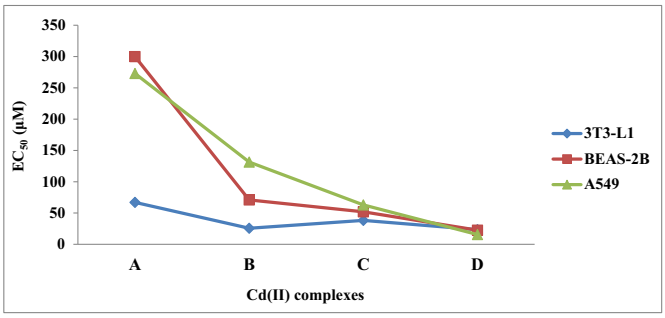

Fig. 11. Plot of EC_{50} change of compounds **1** (**A**), **2** (**B**), **3** (**C**) and **4** (**D**) in the three 3T3-L1, BEAS-2B, and A549 cell lines.

3T3-L1 cell cultures was performed to inquire into the cell migration potential of the title compounds. The results show that cadmium, in both forms employed, induces inhibition of physiological cell migration. More specifically, **1** projected a complete abolishment of migration at the concentration tested (10 μM). In the case of **2**, cells also exhibited reduced migration. An explanation of this result may be linked to the fact that cadmium is thought to influence negatively the physiological wound healing process in vivo via interactions with calcium and zinc [37]. Cell migration is based on the tightly orchestrated action of cytoskeletal components. To that end, it is worth pointing out that cadmium affects the organization of microtubular cytoskeleton in interphase and mitotic cells of *Allium sativum* [38]. Previous work from the lab on cadmium complex influence on cell migration reveals that Cd (II) affects cell motility in a structure-specific manner [27]. Throughout the whole experimental procedure, cells were monitored with respect to cell morphology.

The distinct toxicity behavior of Cd(II), in the form of discrete compounds at the binary-ternary level, necessitated at the outset of the investigation careful assessment of compound profiling prior to proceeding to more in depth studies. In that respect, toxicity studies indicated that ternary compounds **3** and **4** were the most toxic ones, among all four compounds tested. The transition from the binary level of the Cd(II)-(α-hydroxy isubutyrato) systems to the ternary level indicates that introduction of the bulky, hydrophobic, aromatic chelators 2,2′-bipy and phen into the coordination sphere of Cd(II) is linked to enhanced toxicity toward cells exposed to the specific compounds. That, in turn, indicates that the aromatic chelators may be responsible for the enhancement of the observed toxicity, as such ligand binders have been proven in the past to exhibit toxicity toward cellular organisms [39]. Further assertion, however, of the contribution of the individual aromatic chelator to the overall toxicity profile of the binary Cd(II)-(α-hydroxy isobutyrato) system upon entry to the Cd(II) coordination sphere requires further work. In that respect, and to the extent that known cytotoxic profiles of Cd(II) species were required to probe into the behavior of that toxin, compounds **1** and **2** were selected to be employed in the ensuing biological experiments.

4.4. Cytoprotective activity of chelating and antioxidant agents

Following assessment of the cytotoxic potential of **1** and **2** with respect to normal vs cancer state of cells, the potential cytoprotective activity of known antioxidants (N-Acetyl Cysteine, NAC) and chelators (8-hydro-7-iodo-5-sulfonic acid, HO-I-SA) was also examined. Cells were exposed to the aforementioned agents for 1 h and then compounds **1** and **2** were added at the stoichiometric ratio of 1:1 and at concentrations 100 and 500 μM. The specific concentrations were selected on the basis of cell survival data of the preceding experiments. NAC was employed due to its known antioxidant activity, whereas HO-I-SA was used based on its potential to seek metal ion complexation. In fact, the closest structural link to HO-I-SA, clioquinol, is a known effective chelator [40,41] yet it exhibits limited solubility. Thus, HO-I-SA stands as the soluble structural variant of clioquinol at pH 7.4 (Scheme 2).

Prior to assessing the cytoprotective capacity of the two aforementioned agents, their (a)toxic profile was investigated. NAC was completely atoxic at both concentrations tested. HO-I-SA was found to reduce cell viability at high concentration (500 μM) for both cell lines (vide supra). Following treatment, the results show that there is a distinct effect of HO-I-SA on Cd(II)-induced cytotoxicity in both cell lines that clearly depends on the nature of the complex employed (either **1** or **2**). Despite the fact that HO-I-SA alone reduces cell viability after an incubation period of 24 h (vide supra), pre-incubation of cell cultures with HO-I-SA alone over a period of 1 h (significantly shorter period than 24 h) does not inflict damage to cells prior to Cd(II) compound addition to the cell culture, thereby a) standing as a non-toxic viable contender for Cd(II) sequestration, and b) justifying its use in the biological tests carried out on physicochemical grounds (chelation).

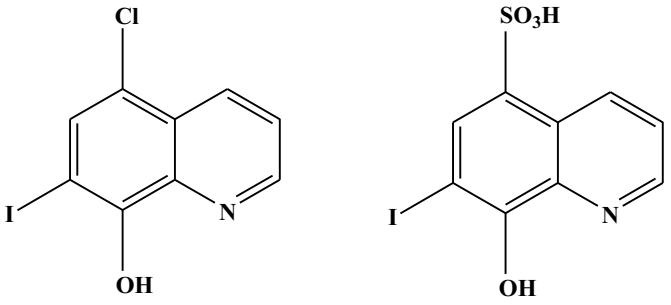

Clioquinol **HO-I-SA**

Scheme 2. Clioquinol variants.

In no case, among the investigated complexes, during the experimental procedures, was there an indication that the examined Cd(II) species had no influence on cell survival. Therefore, the observed bioactivity was commensurate to the nature of the Cd(II) species to which the cells were exposed. Wherever there is interaction (between the chelator and the investigated complex of Cd(II)), viability decreases by 14 to 21% (Tables 3, S3). In the case of compound **1**, and in the case of BEAS-2B cells, the presence of the chelator at 100 μM causes a decrease in cell survival (Tables 3, S3). The chelator itself is a potent binder, with its metal ion complex ability exemplified by the rigidity of the chelation bite formulated by the structure of the quinoline core. To that end, when the chelator is used alone, the possibility of its seeking and pursuing metal ion chelation with metal ions essential to the physiology of the cell is quite realistic. Thus, the emerging effect could be detrimental, essentially contributing to the decrease of cell survival as that is shown in several cases. When the chelator is used in conjunction with the Cd(II):[HIBAH$^-$] complex species, to which the cells are exposed, the possibility that ternary species resulting from the interaction of the chelator and the complex added cannot be excluded, thereby leading to the formation of new species exhibiting a different behavior toward cell survival. The latter behavior is attested to by the increase in cell survival compared to the chelator alone and/or the Cd (II):[HIBAH$^-$] species alone (Tables 3, S3). To that end, the ability of the chelator to intervene, interfere and ultimately provide protection from Cd(II) biochemical activity is ostensible and rides on the relative kinetic and thermodynamic principles characterizing the multitude of interactions evolving through the presence of both the investigated species of Cd(II), the chelator, and the biomolecular targets in the cellular milieu that sustain cell physiology.

5. Conclusions

The importance of well-defined Cd(II) species in a cellular milieu, where toxic manifestations arise, is exemplified through the pH-specific synthetic efforts of binary and ternary systems of Cd(II) with the α-hydroxycarboxylic acid $HIBAH_2$ and the N,N′-aromatic chelators 2,2′-

Table 3
Percent cell survival of **1** and **2** in BEAS-2B and A549 cell lines.

	BEAS-2B		A549	
	HO-I-SA		HO-I-SA	
	100 μM	500 μM	100 μM	500 μM
Compound **1**	X	√	X	√
Compound **2**	√	√	X	X

X = synergistic decrease of cell survival.
√ = increase of cell survival (cytoprotection).

bipy and phen. The physicochemical characterization of crystalline materials **1**–**4** and the associated transformation chemistry between **1** (a coordination polymer) and **2** (a discrete molecular species) revealed the tight association between Cd(II)-forms emerging through chemistry with low molecular mass, physiologically relevant, ligands in aqueous cellular fluids. The physicochemical characteristics of **1**–**4** were employed to further investigate their toxicity profile in three different cell lines (3T3-L1, BEAS-2B and A549) exemplifying structure-, concentration-, and tissue-specific behavior, all important in assessing the exposure of cells to the metallotoxin. Further inquiry into caspase-dependence of toxicity effects on cells shed light onto mechanistic aspects of the cellular demise upon Cd(II) exposure. The ensuing employment of known chelators in Cd(II)-exposed cells revealed the importance of the structure of the chelator and the binding ability of its structural features, enhancing the avidity with which Cd(II) could be sequestered away from toxic manifestations under the influence of competitive interactions (thermodynamic considerations). Ultimately, the work denotes the significance of well-defined forms of Cd(II) in aqueous media, based on which efficient organic chelators could be utilized to specifically bind away Cd(II) without affecting vital functions sustaining cell viability.

Abbreviations

ANOVA	One way analysis of variance
DMEM	Dulbecco's modified Eagle's medium
EC_{50}	50% of the maximum effect concentration
ESI-MS	Electrospray Ionization Mass Spectrometry
FBS	Fetal Bovine Serum
FT-IR	Fourier Transform-Infrared
$HIBAH_2$	α-Hydroxy isobutyric acid
HO-I-SA	8-Hydro-7-iodo-5-sulfonic acid
NAC	N-Acetyl Cysteine
NMR	Nuclear Magnetic Resonance
RLU	Relative Luminescence Units
SEM	Standard error mean
TGA	Thermogravimetric analyses

Acknowledgments

Financial support to C. Iordanidou by “IKY Fellowships of Excellence for Postgraduate studies in Greece–Siemens Program, 2012-2013, Grant No.: SPhD/11236/13β” is acknowledged. The authors also gratefully acknowledge the support and generosity of Scient-Research Center for Instrumental Analysis, by Cromatec Plus SRL, for assisting with thermal analysis.

Appendix A. Supplementary data

CCDC 1856026 (**1**), 1856027 (**2**), 1856028 (**3**), and 1856029 (**4**) contain the supplementary crystallographic data for this paper. These data can be obtained free of charge via www.ccdc.cam.ac.uk/conts/retrieving.html (or from the Cambridge Crystallographic Data Centre, 12 Union Road, Cambridge CB21EZ, UK; fax: (+44) 1223-336-033; or deposit@ccde.cam.ac.uk). Supplementary data to this article can be found online at doi:https://doi.org/10.1016/j.jinorgbio.2019.02.009.

References

[1] E. Borenfreund, J.A. Puerner, Toxicology 39 (1986) 121–134.
[2] S.A. Adefegha, G. Oboh, O.S. Omojokun, O.M. Adefegha, Biomed. Pharmacother. 83 (2016) 559–568.
[3] G. Wang, B.A. Fowler, Tox. Appl. Pharm. 233 (2008) 92–99.
[4] S. Petanidis, M. Hadzopoulou-Cladaras, A. Salifoglou, J. Inorg. Biochem. 121 (2013) 100–107.
[5] Y.-O. Son, L. Wang, P. Poyil, A. Budhraja, J.A. Hitron, Z. Zhang, J.-C. Lee, X. Shia, Tox. Appl. Pharm. 264 (2012) 153–160.
[6] M.A. Pacheco-Blas, H. Dominguez, M. Rivera, Chem. Phys. 485-486 (2017) 13–21.
[7] A. Khalid, I.H. Bukhari, M. Riaz, G. Rehman, Q.U. Ain, T.H. Bokhari, N. Rasool, M. Zubair, S. Munir, IJBPAS 2 (5) (2013) 1003–1009.
[8] Q. Zhai, R. Yin, L. Yu, G. Wang, F. Tian, R. Yu, J. Zhao, X. Liu, Y.Q. Chen, H. Zhang, W. Chen, Food Control 54 (2015) 23–30.
[9] A.R. Nair, O. DeGhesselle, K. Smeets, E. Van Kerkhove, A. Cuypers, Int. J. Mol. Sci. 14 (2013) 6116–6143.
[10] A. Skipper, J.N. Sims, C.G. Yedjou, P.B. Tcounwou, Int. J. Environ. Res. Public Health 13 (2016) 88.
[11] J.D. Henderson, F.P. Filice, M.S.M. Li, Z. Ding, J. Inorg. Biochem. 158 (2016) 92–98.
[12] E.T. Kefalas, M. Dakanali, P. Panagiotidis, C.P. Raptopoulou, A. Terzis, T. Mavromoustakos, I. Kyrikou, N. Karligiano, A. Bino, A. Salifoglou, Inorg. Chem. 44 (2005) 4818–4828.
[13] M.L. Ferramola, M.F.F. Perez Diaz, S.M. Honore, S.S. Sanchez, R.I. Anton, A.C. Anzulovich, M.S. Gimenez, Toxicol. Appl. Pharmacol. 265 (2012) 380–389.
[14] R. Gupta, R.K. Shukla, L.P. Chandravanshi, P. Srivastava, Y.K. Dhuriya, J. Shanker, M.P. Singh, A.B. Pant, V.K. Khanna, Mol. Neurobiol. 54 (6) (2017) 4560–4583.
[15] Z. Wei, X. Song, Z.A. Shaikh, Toxicol. Appl. Pharmacol. 289 (2015) 98–108.
[16] a) S.A. Mouron, C.A. Grillo, F.N. Dulout, C.D. Golijow, Mutat. Res. 568 (2004) 221–231;
b) D. Beyersmann, S. Hechtenberg, Toxicol. Appl. Pharmacol. 144 (2) (1997) 247–261.
[17] P. Joseph, Toxicol. Appl. Pharmacol. 238 (2009) 272–279.
[18] M.D. Pavlaki, M.J. Araujo, D.N. Cardoso, A.R.R. Silva, A. Cruz, S. Mendo, A.M.V.M. Soares, R. Calado, S. Loureiro, Environ. Pollut. 215 (2016) 203–212.
[19] a) E. Halevas, A. Karamelidou, A. Hatzidimitriou, C. Mateescu, A. Salifoglou, Eur. J. Inorg. Chem. (2015) 664–679;
b) Y. Shigematsu, M. Sudo, T. Momoi, Y. Inoue, Y. Suzuki, J. Kameyama, Pediatr. Res. 16 (9) (1982) 771–775;
c) R. Salgado, A. Oehmen, G. Carvalho, J.P. Noronha, M.A.M. Reis, J. Hazardous, Materials 241-242 (2012) 182–189.
[20] Bruker Analytical X-ray Systems, Inc., Apex2, Version 2 User Manual, M86-E01078, Madison, WI, (2006).
[21] Siemens Industrial Automation, Inc., SADABS: Area-Detector Absorption Correction; Madison, WI, (1996).
[22] P.W. Betteridge, J.R. Carruthers, R.I. Cooper, K. Prout, D.J. Watkin, J. Appl. Crystallogr. 36 (2003) 1487.
[23] L. Palatinus, G.J. Chapuis, Appl. Cryst. 40 (2007) 786–790.
[24] DIAMOND, Crystal and Molecular Structure Visualization, Ver. 3.1c, Crystal Impact, Bonn, Germany, (2006).
[25] O. Tsave, M.P. Yavropoulou, M. Kafantari, C. Gabriel, J.G. Yovos, A. Salifoglou, J. Inorg. Biochem. 186 (2018) 217–227.
[26] C. Iordanidou, O. Tsave, C. Gabriel, A. Hatzidimitriou, M.P. Yavropoulou, C. Mateescu, A. Salifoglou, J. Inorg. Biochem. 176 (2017) 38–52.
[27] C. Iordanidou, O. Tsave, C. Gabriel, A. Hatzidimitriou, A. Salifoglou, Inorg. Chim. Acta 482 (2018) 364–374.
[28] S. Chen, G. Liu, M. Long, H. Zou, H. Cui, J. Inorg. Biochem. 184 (2018) 19–26.
[29] M. Dakanali, E.T. Kefalas, C.P. Raptopoulou, A. Terzis, T. Mavromoustakos, A. Salifoglou, Inorg. Chem. 42 (2003) 2531–2537.
[30] a) G.A. Geffrey, Introduction to Hydrogen Bonding, Oxford University Press, New York, 1997;
b) G.A. Geffrey, W. Saenger, Hydrogen Bonding in Biological Structures, Springer-Verlag, Berlin, 1994.
[31] M.P. Barrouilleta, C. Ohayon-Courtès, I. Dubus, B. L'Azou, C. Nguyen Ba, Toxicol. In Vitro 15 (2001) 525–529.
[32] A.A. Tinkov, T. Filippini, O.P. Ajsuvakova, J. Aaseth, Y.G. Gluhcheva, J.M. Ivanova, G. Bjørklund, M.G. Skalnaya, E.R. Gatiatulina, E.V. Popova, O.N. Nemereshina, M. Vinceti, A.V. Skalny, Sci. Total Environ. 601–602 (2017) 741–755.
[33] M. Brama, L. Politi, P. Santini, S. Migliaccio, R. Scandurra, J. Endocrinol. Investig. 35 (2) (2012) 198–208.
[34] N. Ataei, M. Aghaei, M. Panjehpour, Res. Pharm. Sci. 13 (2) (2018) 159–167.
[35] a) A. Hartwig, Met. Ions Life Sci. 11 (2013) 491–507;
b) M. Feki-Tounsi, A. Hamza-Chaffai, Environ. Sci. Pollut. Res. Int. 18 (2014) 10561–10573.
[36] G. Jiang, W. Duan, L. Xu, S. Song, C. Zhu, L. Wu, Toxicol. In Vitro 23 (6) (2009) 973–978.
[37] A.B. Lansdown, B. Sampson, A. Rowe, Int. J. Exp. Pathol. 82 (1) (2001) 35–41.
[38] P. Xu, D. Liu, W. Jiang, Biol. Plant. 53 (2009) 387–390.
[39] L.W. Scheibel, A. Adler, Mol. Pharmacol. 18 (2) (1980) 320–325.
[40] M.J. Pushie, K.H. Nienaber, K.L. Summers, J.J.H. Cotelesage, O. Ponomarenko, H.K. Nichol, I.J. Pickering, G.N. George, J. Inorg. Biochem. 133 (2014) 50–56.
[41] M. Di Vaira, C. Bazziculpi, P. Orioli, L. Messori, B. Bruni, P. Zatta, Inorg. Chem. 43 (2004) 3795–3797.